

Manuscript version: Author's Accepted Manuscript

The version presented in WRAP is the author's accepted manuscript and may differ from the published version or Version of Record.

Persistent WRAP URL:

<http://wrap.warwick.ac.uk/113199>

How to cite:

Please refer to published version for the most recent bibliographic citation information. If a published version is known of, the repository item page linked to above, will contain details on accessing it.

Copyright and reuse:

The Warwick Research Archive Portal (WRAP) makes this work by researchers of the University of Warwick available open access under the following conditions.

Copyright © and all moral rights to the version of the paper presented here belong to the individual author(s) and/or other copyright owners. To the extent reasonable and practicable the material made available in WRAP has been checked for eligibility before being made available.

Copies of full items can be used for personal research or study, educational, or not-for-profit purposes without prior permission or charge. Provided that the authors, title and full bibliographic details are credited, a hyperlink and/or URL is given for the original metadata page and the content is not changed in any way.

Publisher's statement:

Please refer to the repository item page, publisher's statement section, for further information.

For more information, please contact the WRAP Team at: wrap@warwick.ac.uk.

THE EFFECT OF CRYSTAL SYMMETRIES ON THE LOCALITY OF SCREW DISLOCATION CORES*

JULIAN BRAUN[†], MACIEJ BUZE[†], AND CHRISTOPH ORTNER[†]

Abstract. In linearised continuum elasticity, the elastic strain due to a straight dislocation line decays as $O(r^{-1})$, where r denotes the distance to the defect core. It is shown in [8] that the *core correction* due to nonlinear and discrete (atomistic) effects decays like $O(r^{-2})$.

In the present work, we focus on screw dislocations under pure anti-plane shear kinematics. In this setting we demonstrate that an improved decay $O(r^{-p})$, $p > 2$, of the core correction is obtained when crystalline symmetries are fully exploited and possibly a simple and explicit correction of the continuum far-field prediction is made.

This result is interesting in its own right as it demonstrates that, in some cases, continuum elasticity gives a much better prediction of the elastic field surrounding a dislocation than expected, and moreover has practical implications for atomistic simulation of dislocations cores, which we discuss as well.

Key words. screw dislocations, anti-plane shear, lattice models, regularity, defect core

AMS subject classifications. 35Q74, 49N60, 70C20, 74B20, 74G10, 74G65

1. Introduction. Crystalline solids consist of regions of periodic atom arrangements, which are broken by various types of defects. Crystalline defects can be separated into an elastic far-field which can normally be described by continuum linearised elasticity (CLE) and a defect core which is inherently atomistic and determines, for example, mobility, formation energy (and hence concentration), and so forth.

To make this idea concrete, let $\Lambda \subset \mathbb{R}^d$ be a crystalline lattice reference configuration and let $u : \Lambda \rightarrow \mathbb{R}^d$ be an equilibrium displacement field under some interaction law (see § 2.1). The point of view advanced in [8] is to decompose $u = u_{\text{ff}} + u_{\text{core}}$ where u_{ff} is a *far-field predictor* solving a CLE equation enforcing the presence of the defect of interest and u_{core} is a *core corrector*. For example, it is shown in [8] that for dislocations $|Du_{\text{ff}}(x)| \sim |x|^{-1}$ while $|Du_{\text{core}}(x)| \lesssim |x|^{-2} \log |x|$ where D denotes a discrete gradient operator. The fast decay of the corrector u_{core} encodes the “locality” of the defect core (relative to the far-field).

The present work is the first in a series that introduces and develops techniques to substantially improve on the CLE far-field description. The overarching goal is to derive “higher-order” models for the far-field predictor u_{ff} , which yield the same asymptotic behaviour as the CLE predictor (i.e., the same far-field boundary condition) but a more localised corrector. For example, in the case of a dislocation we seek u_{ff} such that $u = u_{\text{ff}} + u_{\text{core}}$ with $|Du_{\text{core}}(x)| \lesssim |x|^{-p}$ and $p > 2$. Constructions of this kind have a multitude of applications. They are interesting in their own right in that they give improved estimates on the region of validity of continuum mechanics. They may also be employed to more effectively construct models for multiple defects along the lines of [12]. A key motivation for us is that they yield a new class of boundary conditions for atomistic simulations that capture the far-field behaviour more accurately; this gives rise to improved algorithms for atomistic simulation defects; see § 3 for more detail.

In the present work, to demonstrate the potential of our approach and outline

*Submitted to the editors 17th November 2017.

Funding: MB is supported by EPSRC as part of the MASDOC DTC, Grant No. EP/HO23364/1. JB and CO are supported by ERC Starting Grant 335120.

[†]Mathematics Institute, University of Warwick, Coventry, CV4 7AL, UK.

44 some of the key ideas required to carry out this programme, we focus on screw dislo-
 45 cations under anti-plane shear kinematics, in the cubic, hexagonal, and body-centred-
 46 cubic (BCC) lattices. The scalar setting, and the ability to exploit specific lattice
 47 symmetries, simplifies several constructions and proofs.

48 In forthcoming papers, in particular [2], we will discuss generalisations to vectorial
 49 deformations of general straight dislocations without any symmetry assumptions on
 50 the host crystal. In particular the absence of the symmetries we employ in the present
 51 work introduces a non-trivial coupling between the core and the far-field predictor. The
 52 general idea that persists is that there is a development $u = u_0 + u_1 + \dots + u_n + u_{\text{rem}}$
 53 of the solution, where the terms u_0, u_1, \dots, u_n are given by simpler theories (e.g., linear
 54 PDEs) and the remainder u_{rem} has a higher decay rate.

55 Aside from providing a simplified introduction to [2], the present work contains
 56 results that are interesting in their own right due to the fact that anti-plane models
 57 of screw dislocations are particularly popular in the mathematical analysis literature
 58 [1, 10, 12, 18] as a model problem for the more complex edge, mixed, and curved
 59 dislocations. Of particular note about our results here are:

60 (1) Rotational and anti-plane reflection symmetries for both the model and the
 61 equilibrium u yield surprisingly high decay of the core corrector to the CLE predictor;
 62 see Theorem 2.5. This was numerically observed but unexplained in [12]. The key
 63 observation to obtain this result is that the CLE predictor satisfies additional PDEs,
 64 in particular the minimal surface equation, which naturally occurs in higher-order
 65 expansions of the atomistic forces.

66 (2) In a BCC crystal, due to the lack of anti-plane reflection symmetry, a nonlin-
 67 ear correction to the far-field predictor is required to improve the decay of the core
 68 corrector. One then expects that the dominant error contribution is the Cauchy–Born
 69 anti-discretisation error. The results of [3, 6, 16] suggest that the resultant correc-
 70 tor should decay as $O(|x|^{-3})$, however exploiting crystal symmetries reveals that the
 71 Cauchy–Born error is of higher order than expected and one even obtains a corrector
 72 decay of $O(|x|^{-4})$.

73 In both (1) and (2), due to the high degree of non-convexity in the potential
 74 energy landscape, the required symmetry on the solution u must be an assumption,
 75 but cannot in general be proven. However, at least for potential energy minimisers it
 76 is entirely natural as we argue in Remark 2.4.

77 Finally, we remark that our analysis is carried out for short-ranged interatomic
 78 many-body potentials, however the resulting algorithms are applicable to electronic
 79 structure models rendering them an efficient and attractive alternative to complex
 80 and computationally expensive multi-scale schemes e.g. of atomistic/continuum or
 81 QM/MM type; see [5, 15] and references therein.

82 **Outline:** In Section 2 we describe in details our models and assumptions, and
 83 state our main results. Here, Section 2.2 is dedicated to the cubic and hexagonal
 84 lattice, while Section 2.3 discusses the BCC lattice. In Section 3 we present the
 85 resulting new numerical scheme including a convergence analysis. Our conclusions
 86 can be found in Section 4. Finally Section 5 contains the proofs of the main results.

87 2. Main results.

88 **2.1. Atomistic model for a screw dislocation.** The atomistic reference con-
 89 figuration for a straight screw dislocation is given by a two-dimensional Bravais lattice
 90 $\Lambda = A_\Lambda \mathbb{Z}^2$, $A_\Lambda \in \mathbb{R}^{2 \times 2}$ with $\det(A_\Lambda) \neq 0$. In the present work we will only consider

91 the triangular lattice and the square lattice, respectively given by

$$92 \quad A_\Lambda = A_{\text{tri}} := \begin{pmatrix} 1 & \frac{1}{2} \\ 0 & \frac{\sqrt{3}}{2} \end{pmatrix}, \quad A_\Lambda = A_{\text{quad}} := \begin{pmatrix} 1 & 0 \\ 0 & 1 \end{pmatrix}.$$

93 The two-dimensional lattice Λ should be thought of as the projection of a three-
94 dimensional lattice: In case of an infinite straight dislocation in a three-dimensional
95 lattice, the displacements do not depend on the dislocation line direction. Therefore,
96 it suffices to consider the projected two-dimensional lattice.

97 Our atomistic model, which we specify momentarily, allows for general finite range
98 interactions. All lattice directions included in the interaction range are encoded in a
99 finite neighbourhood set $\mathcal{R} \subset \Lambda \setminus \{0\}$, which is fixed throughout. We always assume
100 $\text{span}_{\mathbb{Z}} \mathcal{R} = \Lambda$ and will specify further symmetry assumptions later on.

101 We consider an anti-plane displacement field $u : \Lambda \rightarrow \mathbb{R}$ and define $D_\rho u(x) :=$
102 $u(x + \rho) - u(x)$, $Du(x) := (D_\rho u(x))_{\rho \in \mathcal{R}}$, as well as the discrete divergence operator,

$$103 \quad \text{Div } g(x) := - \sum_{\rho \in \mathcal{R}} g_\rho(x - \rho) - g_\rho(x) \quad \text{for any } g : \Lambda \rightarrow \mathbb{R}^{\mathcal{R}}.$$

104 In contrast to that we will always write ∇ and div if we talk about the standard
105 (continuum) gradient and divergence of differentiable maps.

106 A suitable function space for (relative) displacements is

$$107 \quad \dot{\mathcal{H}}^1 := \{u : \Lambda \rightarrow \mathbb{R} \mid Du \in \ell^2(\Lambda)\} / \mathbb{R},$$

108 with norm

$$109 \quad \|u\|_{\dot{\mathcal{H}}^1} := \left(\sum_{x \in \Lambda} |Du(x)|^2 \right)^{1/2}.$$

110 While we have factored out constants to make this a Banach space, we will often use
111 the displacement u and its equivalence class $[u]$ interchangeably when there is no risk
112 of confusion.

113 For analytical purposes, we will also consider the space of compactly supported
114 displacements

$$115 \quad \mathcal{H}^c := \{u : \Lambda \rightarrow \mathbb{R} \mid \text{spt}(u) \text{ is bounded}\}.$$

116 Displacement fields containing dislocations do not belong to $\dot{\mathcal{H}}^1$ and the energy,
117 naively written as a sum of local contributions, will be infinite. Following [8, 12] we
118 therefore consider energy differences

$$119 \quad (1) \quad \mathcal{E}(u) = \sum_{x \in \Lambda} \left(V(D\hat{u}(x) + Du(x)) - V(D\hat{u}(x)) \right),$$

120 where \hat{u} is a chosen *far-field predictor* that encodes the far-field boundary condition,
121 while $u \in \dot{\mathcal{H}}^1$ is a *core corrector* to the given predictor so that $\hat{u} + u$ gives the overall
122 displacement. We will minimise $\mathcal{E}(u)$ to equilibrate the defective crystal, but this
123 requires some preparation first.

124 We assume throughout that $V \in C^6(\mathbb{R}^{\mathcal{R}}, \mathbb{R})$ is a many-body potential encoding
125 the local interactions. Examples of typical site potentials V include Lennard-Jones
126 type pair potentials (with cut-off) and EAM potentials; see also [Section 2.3](#) and
127 [Section 3](#). With significant additional effort it would be possible to include simple
128 quantum chemistry models (e.g. tight binding) within the framework [4]. As discussed

129 in detail in [4] this leads to a model as described above with potentials V that have
 130 infinite range and strong decay estimates. To keep the presentation and calculations
 131 as simple as possible and focus on the topic of symmetry we will not pursue this in
 132 the current work.

133 As Λ is either the square or triangular lattice, which are both invariant under
 134 certain symmetries, one is tempted to directly translate these symmetries to \mathcal{R} and V .
 135 However, as mentioned above, Λ should be seen as a projection of a three-dimensional
 136 lattice. Such a projection can add symmetries for the lattice that are not reflected
 137 in the interaction, since they are not symmetries of the underlying three-dimensional
 138 model. We will discuss such a case in detail in [Section 2.3](#).

139 Because of this, we will only make the following reduced symmetry assumptions
 140 on \mathcal{R} and V throughout. Let Q_Λ be the rotation by $\pi/2$ if $\Lambda = \mathbb{Z}^2$ and the rotation
 141 by $2\pi/3$ if $\Lambda = A_{\text{tri}}\mathbb{Z}^2$. Then we assume that

$$142 \quad (2) \quad Q_\Lambda \mathcal{R} = \mathcal{R} \quad \text{and} \quad V(A) = V((A_{Q_\Lambda \rho})_{\rho \in \mathcal{R}}) \quad \forall A \in \mathbb{R}^{\mathcal{R}}.$$

143 Since we only consider a plane orthogonal to the direction of the dislocation line,
 144 it is natural that the energy does not change if the displacements shifts an atom to
 145 its equivalent position in the plane above or below. Indeed we assume that there is a
 146 minimal periodicity $p > 0$ such that

$$147 \quad V(A) = V(A + p(\delta_{\rho\sigma})_{\sigma \in \mathcal{R}}) \quad \text{for all } A \in \mathbb{R}^{\mathcal{R}}, \quad \rho \in \mathcal{R},$$

148 where δ is the Kronecker delta. The Burgers vector of a screw dislocation is then
 149 either $b = p$ or $b = -p$.

150 A key conceptual assumption that we require throughout this work is lattice
 151 stability (or, phonon stability): there exists $c_0 > 0$ such that

$$152 \quad (3) \quad \langle Hu, u \rangle \geq c_0 \|u\|_{\mathcal{H}^1}^2 \quad \forall u \in \hat{\mathcal{H}}^1,$$

153 where H denote the Hessian of the potential energy evaluated at the homogeneous
 154 lattice (note that this is different from $\delta^2 \mathcal{E}(0)$),

$$155 \quad \langle Hu, v \rangle = \sum_{x \in \Lambda} \sum_{\rho, \sigma \in \mathcal{R}} \nabla^2 V(0)_{\rho\sigma} D_\rho u(x) D_\sigma v(x), \quad \text{for } u, v \in \hat{\mathcal{H}}^1.$$

156 The choice of the predictor \hat{u} in (1) for a specific problem is part of the modelling
 157 since it determines the far-field behaviour, e.g., it could encode an applied strain.
 158 Intuitively one can obtain a suitable \hat{u} by solving a ‘‘simpler’’ model such as continuum
 159 linearised elasticity (CLE), which one expects to be approximately valid in the far-
 160 field; see [8] for a formalisation of this procedure.

161 Assume, for the time being, that $\hat{u} : \mathbb{R}^2 \rightarrow \mathbb{R}$ is smooth away from a defect core
 162 $\hat{x} \in \mathbb{R}^2 \setminus \Lambda$. Then, by employing Taylor expansions of both \hat{u} and of V , we can
 163 approximate the atomistic force,

$$164 \quad \left. \frac{\partial \mathcal{E}}{\partial u(x)} \right|_{u=0} = \left(-\text{Div } \nabla V(D\hat{u}) \right)(x)$$

$$165 \quad (4) \quad = -c \text{div } \nabla W(\nabla \hat{u}) + O(\nabla^4 \hat{u}(x)) + \text{h.o.t.s}$$

$$166 \quad = -c \text{div}(\nabla^2 W(0)[\nabla \hat{u}]) + O(\nabla^4 \hat{u}) + O(\nabla^2 \hat{u} \nabla \hat{u}) + \text{h.o.t.s},$$

168 where $c = \det A_\Lambda$ and $W : \mathbb{R}^2 \rightarrow \mathbb{R}$ is the *Cauchy–Born energy per unit undeformed*
 169 *volume*, defined by

$$170 \quad (5) \quad W(F) := \frac{1}{\det A_\Lambda} V(F \cdot \mathcal{R}),$$

171 with the notation $(F \cdot \mathcal{R})_\rho = F \cdot \rho$. Moreover, $O(\nabla^4 \hat{u})$ represents the *anti-discretisation*
 172 *error* (note that the continuum model is now the approximation), $O(\nabla^2 \hat{u} \nabla \hat{u})$ the
 173 linearisation error and “h.o.t.s” denotes additional terms that will be negligible in
 174 comparison.

175 It is therefore natural to solve a CLE model to obtain a far-field predictor for the
 176 atomistic defect equilibration problem for an anti-plane screw dislocation. Let $\hat{x} \in \mathbb{R}^2$
 177 denote the dislocation core, then we define the branch cut (slip plane)

$$178 \quad \Gamma := \{(x_1, \hat{x}_2) \in \mathbb{R}^2 \mid x_1 \geq \hat{x}_1\}$$

179 and solve (we will see in [Corollary 5.4](#) that under our general assumptions on \mathcal{R} and
 180 V we have $\nabla^2 W(0) \propto \text{Id}$)

$$181 \quad (6a) \quad -\Delta \hat{u} = 0 \quad \text{in } \mathbb{R}^2 \setminus \Gamma,$$

$$182 \quad (6b) \quad \hat{u}(x^+) - \hat{u}(x^-) = -b \quad \text{on } \Gamma \setminus \hat{x},$$

$$183 \quad (6c) \quad \partial_{x_2} \hat{u}(x^+) - \partial_{x_2} \hat{u}(x^-) = 0 \quad \text{on } \Gamma \setminus \hat{x}.$$

185 The system [Eq. \(6a\)–Eq. \(6c\)](#) has the well-known solution (cf. [\[9\]](#))

$$186 \quad (7) \quad \hat{u}(x) = \frac{b}{2\pi} \arg(x - \hat{x}),$$

187 where we identify $\mathbb{R}^2 \cong \mathbb{C}$ and use $\Gamma - \hat{x}$ as the branch cut for \arg . Note for later use,
 188 that $\nabla \hat{u} \in C^\infty(\mathbb{R}^2 \setminus \{0\})$ and $|\nabla^j \hat{u}| \lesssim |x|^{-j}$ for all $j \geq 0$ and $x \neq 0$.

189 As we want to study the effects of symmetry, we will assume throughout that the
 190 dislocation core \hat{x} is, respectively, at the center of a triangle or square.

191 Having specified the far-field predictor we can now recall properties of the resulting
 192 variational problem.

193 **PROPOSITION 2.1.** *Let \hat{u} be given by [\(7\)](#), then \mathcal{E} defined by [\(1\)](#) on \mathcal{H}^c has a unique*
 194 *continuous extension $\mathcal{E}: \dot{\mathcal{H}}^1 \rightarrow \mathbb{R}$. Furthermore, $\mathcal{E} \in C^6(\dot{\mathcal{H}}^1)$.*

195 *Proof.* This is proven in [\[8, Lemma 3 and Remark 6\]](#). □

196 Having established that \mathcal{E} is well-defined, it is now meaningful to discuss the
 197 equilibration problem, either energy minimisers

$$198 \quad (8) \quad \bar{u} \in \arg \min_{\dot{\mathcal{H}}^1} \mathcal{E}$$

199 or, more generally, critical points

$$200 \quad \delta \mathcal{E}(\bar{u}) = 0.$$

201 Critical points of the energy satisfy the following regularity and decay estimate.

202 **THEOREM 2.2.** *If $[\bar{u}] \in \dot{\mathcal{H}}^1$ is a critical point of \mathcal{E} , then there exists $\bar{u}_\infty \in \mathbb{R}$ such*
 203 *that*

$$204 \quad |D^j(\bar{u}(x) - \bar{u}_\infty)| \lesssim |x|^{-j-1} \log|x|,$$

205 for all $|x|$ large enough and $0 \leq j \leq 4$.

206 *Proof.* This result is proven in [\[8, Theorem 5 and Remark 9\]](#). □

2.2. Anti-plane screw dislocations with mirror symmetry. The corrector decay rates in [8] are in general sharp (up to constants and log-factors), however the case of anti-plane screw dislocations appears to be an exception: In [12] it is seen numerically for a triangular lattice that, if the core is placed at the centre of a triangle, one approximately has $|Du(x)| \sim |x|^{-4}$ instead of the expected rate $|x|^{-2} \log|x|$. In the present section we relate this observation to several symmetry properties of the triangular lattice. We also discuss the square lattice case which shows a different behaviour to emphasise the importance of the triangular lattice.

These two-dimensional models represent a screw-dislocation in a cubic or hexagonal three-dimensional lattice only allowing for anti-plane displacements. In Section 2.3, we will additionally consider a BCC lattice and show how to derive these two-dimensional systems from the underlying three-dimensional model.

We recall that Λ is either the square or triangular lattice which are both invariant under certain rotational symmetries. Crucially, we consider rotations about the dislocation core (not about a lattice site), which are described by the operators

$$L_\Lambda x := Q_\Lambda(x - \hat{x}) + \hat{x},$$

where Q_Λ denotes a rotation through $\pi/2$ if $\Lambda = \mathbb{Z}^2$ and a rotation through $2\pi/3$ if $\Lambda = A_{\text{tri}}\mathbb{Z}^2$. Since we assumed that \hat{x} lies, respectively, at a center of triangle or square this implies $L_\Lambda\Lambda = \Lambda$.

In the present section we additionally assume mirror symmetry with respect to the plane orthogonal to the dislocation line, which is encoded in the site energy through the assumption

$$(9) \quad V(A) = V(-A) \quad \text{for all } A \in \mathbb{R}^{\mathcal{R}}.$$

The mirror symmetry (9) is already implicit in our general assumptions for the square lattice (as it can be decomposed into a point reflection and an in-plane rotation by π). But it is an additional assumption for the triangular lattice. Here, it is equivalent to strengthen the rotational symmetry to rotations by $\pi/3$ instead of just $2\pi/3$.

Since A represents an anti-plane *displacement gradient* Du , the map $A \mapsto -A$ does not represent a change in frame as it would in a full three-dimensional setting. In particular the derivation of V for the BCC case in Section 2.3 shows that (9) is a non-trivial restriction on V .

Indeed, if one derives V from an underlying three-dimensional site potential (see Section 2.3 for such a derivation in the case of a BCC lattice), then (9) means precisely that the three-dimensional lattice is mirror symmetric with respect to the plane orthogonal to the dislocation line. This is quite restrictive and effectively only true if the underlying three-dimensional lattice is given as $\Lambda' = \Lambda \times \mathbb{Z} \subset \mathbb{R}^3$ which is a hexagonal or a cubic lattice for $\Lambda = A_{\text{tri}}\mathbb{Z}^2$ or $\Lambda = \mathbb{Z}^2$, respectively.

In the next section Section 2.3, we will then consider a situation where (9) fails, by discussing a 111 screw dislocation in a BCC lattice.

Recall from (7) that the far-field predictor is given by $\hat{u}(x) = \frac{b}{2\pi} \arg(x - \hat{x})$. Since we now assume that \hat{x} is at the centre of a square or triangle, \hat{u} satisfies

$$(10) \quad \hat{u}(L_\Lambda x) = \begin{cases} \hat{u}(x) + \frac{b}{3} \pmod{b}, & \text{triangular lattice,} \\ \hat{u}(x) + \frac{b}{4} \pmod{b}, & \text{square lattice.} \end{cases}$$

Motivated by this observation, we specify an analogous symmetry *assumption* on a general displacement.

253 DEFINITION 2.3 (Inheritance of symmetries). *We say that a displacement u in-*
 254 *herits the rotational symmetry of \hat{u} if*

$$255 \quad (11) \quad u(L_\Lambda x) = u(x) \quad \text{for all } x \in \Lambda.$$

256 *Remark 2.4.* Inheritance of rotational (or other) symmetries would typically fol-
 257 low from the corresponding symmetries of \hat{u}, Λ, V and uniqueness of an energy min-
 258 imiser (up to a global translation and lattice slips). However, due to the severe
 259 non-convexity of the energy landscape uniqueness cannot be expected in general. As
 260 an example, note that the line reflection symmetry in the BCC case, discussed in
 261 [Section 2.3](#), is not necessarily inherited as is shown in [\[19\]](#).

262 We can now state the main results of this section. It is particularly noteworthy
 263 that they depend on the lattice under consideration. On a square lattice the symmetry
 264 only gives one additional order of decay compared to the decay rates in [\[8\]](#), while on a
 265 triangular lattice we do indeed show that there are two additional orders of decay as
 266 observed numerically in [\[12, Remark 3.7\]](#). While the lattice symmetries in both cases
 267 lead to isotropic linear elasticity as a first approximation, we will show that higher-
 268 order terms show anisotropies depending on the underlying lattice (see [Lemma 5.2](#))
 269 which in turn lead to the different decay rates here. We will confirm this discrepancy
 270 in numerical tests in [Section 3](#).

271 THEOREM 2.5 (Decay with Mirror Symmetry). *Let $\Lambda \in \{\mathbb{Z}^2, A_{\text{tri}}\mathbb{Z}^2\}$ and sup-*
 272 *pose $\Lambda, \hat{x}, \mathcal{R}, V$ satisfy all the assumptions from [Section 2.1](#). Furthermore, assume*
 273 *V satisfies the mirror symmetry [\(9\)](#). If \bar{u} is a critical point of \mathcal{E} which inherits the*
 274 *rotational symmetry of \hat{u} , then we have for $j = 1, 2$ and all $|x|$ large enough*

$$275 \quad (12) \quad |D^j \bar{u}(x)| \lesssim |x|^{-2-j} \log|x|,$$

276 *if $\Lambda = \mathbb{Z}^2$, and*

$$277 \quad (13) \quad |D^j \bar{u}(x)| \lesssim |x|^{-3-j}$$

278 *for the triangular lattice $\Lambda = A_{\text{tri}}\mathbb{Z}^2$.*

279 *Remark 2.6.* The result is also expected to hold for $j \geq 3$ and $j = 0$ (up to
 280 subtracting a constant) following ideas in [\[8\]](#). As we want to focus on other aspects
 281 and do not want to overburden the proof, this is omitted here.

282 *Remark 2.7.* In the case of a triangular lattice the existence of a critical point u
 283 has been proven in [\[12\]](#) under restrictions on V . Under further restrictions it is even
 284 known to be a stable global minimiser. However it is unclear whether the minimizer
 285 is unique or inherits the symmetry. In [Section 3.2](#), we will give numerical evidence for
 286 the decay rates in [\(12\)](#) and [\(13\)](#), thus supporting the conjecture that there are energy
 287 minimisers inheriting the symmetry in these specific models.

288 *Remark 2.8.* We also want to emphasize, that the distinction between the hexag-
 289 onal and BCC lattices, that is the loss of mirror symmetry in the BCC lattice, was
 290 missed in [\[12\]](#). Therefore, the results of [\[12\]](#) do not apply to the BCC case without
 291 further work.

292 *Idea of the proof of [Theorem 2.5](#).* The full proof can be found in [Section 5](#); here
 293 we only give a brief idea of the strategy.

294 Far from the defect core the equilibrium configuration is close to a homogeneous
 295 lattice, hence, the linearised problem becomes a good approximation. Therefore, a

296 natural quantity to consider is the *linear residual*

$$297 \quad (14) \quad f_u = -\operatorname{Div}(\nabla^2 V(0)[Du]).$$

298 On the one hand, one can recover \bar{u} as a lattice convolution $\bar{u} = G *_{\Lambda} f_{\bar{u}}$ where G is
 299 the fundamental solution, or Green's function, of the linear atomistic equations. On
 300 the other hand, the decay of $f_{\bar{u}}$ can be estimated by Taylor expansion with the help
 301 of the nonlinear atomistic equations for $\hat{u} + \bar{u}$ and the continuum linear system for
 302 \hat{u} . In this expansion, $\nabla^3 V(0) = 0$ vanishes due to anti-plane symmetry, while the
 303 rotational symmetry leads to simple generic forms of higher order terms.

304 But even if $f_{\bar{u}}$ decays rapidly, this does not automatically translate to decay for
 305 $\bar{u} = G * f_{\bar{u}}$. Even if $f_{\bar{u}}$ has compact support \bar{u} typically only inherits the decay of G .
 306 However, we show that, due to rotational symmetry, the first moment of $f_{\bar{u}}$ vanishes,
 307 while the second has a very special form. Improved estimates for the decay of $f_{\bar{u}}$
 308 together with vanishing moments then lead to an improved rate of decay of \bar{u} .

309 The difference between the triangular lattice and the quadratic lattice lies in the
 310 form of the higher order terms in the expansion of $f_{\bar{u}}$. The terms in question are
 311 given by the atomistic-continuum error of the linear equation and by the nonlinearity
 312 $\nabla^4 V(0)$. For the triangular lattice one finds the leading order expression $c_1 \Delta^2 \hat{u}$ for the
 313 linear and $c_2(g(x)\Delta \hat{u} + H(\hat{u}))$ for the nonlinear part, where only the constants c_1, c_2
 314 depend on the potentials. Here H is the mean curvature of the graph $(x_1, x_2, \hat{u}(x))^T$.
 315 And the mean curvature vanishes as the graph is a helicoid, a minimal surface. Since
 316 $\Delta^2 \hat{u} = 0$, $\Delta \hat{u} = 0$, and $H(\hat{u}) = 0$ all the leading order terms vanish. On the other
 317 hand, for the quadratic lattice, these terms are nontrivial and do not cancel. \square

318 **2.3. Anti-plane screw dislocation in BCC.** We turn towards the physically
 319 more important setting of a straight screw dislocation along the 111 direction in a
 320 BCC crystal. The three-dimensional BCC lattice can be defined by $\Lambda'' = \mathbb{Z}^3 + \{0, p\}$,
 321 with shift $p = \frac{1}{2}(1, 1, 1)^T$. A screw dislocation along the 111 direction is obtained by
 322 taking both dislocation line and Burgers vector parallel to the vector $(1, 1, 1)^T$. If we
 323 rotate Λ'' by

$$324 \quad Q = \frac{1}{\sqrt{6}} \begin{pmatrix} -1 & -1 & 2 \\ \sqrt{3} & -\sqrt{3} & 0 \\ \sqrt{2} & \sqrt{2} & \sqrt{2} \end{pmatrix}$$

325 and then rescale the lattice by $\sqrt{3/2}$, we obtain the three-dimensional Bravais lattice

$$326 \quad \Lambda' = \sqrt{3/2} Q \Lambda'' = \begin{pmatrix} 1 & \frac{1}{2} & 0 \\ 0 & \frac{\sqrt{3}}{2} & 0 \\ \frac{1}{2\sqrt{2}} & -\frac{1}{2\sqrt{2}} & \frac{3}{2\sqrt{2}} \end{pmatrix} \mathbb{Z}^3.$$

327 The 111 direction becomes the e_3 direction under this transformation, which is con-
 328 venient for the subsequent discussion.

329 Since $p = \frac{3}{2\sqrt{2}}$, the *Burgers vector* is now given by $b = \pm \frac{3}{2\sqrt{2}}$ (corresponding to
 330 the actual *Burgers vector* in three dimensions being $(0, 0, b)^T$). We project the BCC
 331 lattice Λ' along the dislocation direction e_3 to obtain the triangular lattice

$$332 \quad \Lambda = \{(x_1, x_2)^T \mid x \in \Lambda'\} = A_{\text{tri}} \mathbb{Z}^2.$$

333 Note though that these projections correspond to different "heights", i.e., different
 334 z -coordinates in Λ' . Indeed, it is helpful to split Λ into the three lattices $\Lambda = \Lambda_1 \cup$

335 $\Lambda_2 \cup \Lambda_3$, where

336
$$\Lambda_i = v_i + \begin{pmatrix} \frac{3}{2} & \frac{3}{2} \\ \frac{\sqrt{3}}{2} & -\frac{\sqrt{3}}{2} \end{pmatrix} \mathbb{Z}^2,$$

337 with $v_1 = 0$, $v_2 = e_1$, $v_3 = (\frac{1}{2}, \frac{\sqrt{3}}{2})^T$. In this notation, one can recover the three-
 338 dimensional lattice as

339
$$\Lambda' = \bigcup_i \left(\Lambda_i \times \left\{ \left(k + \frac{i}{3} \right) \frac{3}{2\sqrt{2}} : k \in \mathbb{Z} \right\} \right).$$

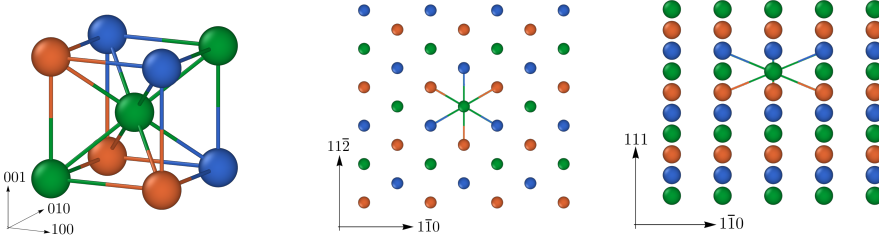


FIG. 1. Consider the middle green atom in the BCC unit cube (left picture). After projecting along the 111-direction (the green diagonal), the three green atoms are represented as one, which has six other-coloured atoms in the unit cube as its nearest-neighbours (middle picture). The different heights of atomic planes associated with each colour are best seen by projecting the same lattice along the 112-direction (right picture).

340 Next, we formally derive an anti-plane interatomic potential as a projection from a
 341 three-dimensional model. The derivation is only formal as many of the sums appearing
 342 are infinite if summed over the entire lattice. Indeed, for a deformation y consider
 343 formally

344
$$\mathcal{E}^{3d}(y) = \sum_{x \in \Lambda'} V'(D'y(x)),$$

345 where $D'y(x) = (D_\rho y(x))_{\rho \in \Lambda'}$ and $V': \mathbb{R}^{3 \times \Lambda'} \rightarrow \mathbb{R}$. Note that, to achieve the pe-
 346 riodicity of V (slip invariance) V' must depend on the entire crystal. However, it
 347 is convenient to assume that it has a finite cut-off $d > 0$ such that $V'(A) = V'(B)$
 348 whenever A, B satisfy $A_\rho = B_\rho$ for all ρ with $|A_\rho| < d$ or $|B_\rho| < d$.

349 In contrast to \mathcal{E} , \mathcal{E}^{3d} acts on deformations instead of displacements. To derive an
 350 energy on anti-plane displacements, we consider deformations of the form

351
$$y^u : \Lambda' \rightarrow \mathbb{R}^3, \quad y^u(x) := (x_1, x_2, x_3 + u(x_1, x_2))^T$$

352 for anti-plane displacements $u : \Lambda \rightarrow \mathbb{R}$. As differences of y^u do not depend on x_3 , the
 353 same is true for the local energy contributions. Therefore, we can formally renormalise
 354 the (possibly infinite) energy to

355
$$\mathcal{E}_{\text{norm}}^{3d}(u) = \sum_{x \in \Lambda' \cap (\mathbb{R}^2 \times [0, p])} V'(D'y^u(x)),$$

356 the energy per periodic layer of thickness p . Since $|D_\rho y^u(x)| \geq |(\rho_1, \rho_2)|$, the local
 357 energy at any x can only depend on the projected directions $\mathcal{R} := \Lambda \cap B_d(0) \setminus \{0\}$. We
 358 can therefore define

359
$$V(Du(x_1, x_2)) := V'(D'y^u(x)),$$

360 for $x \in \Lambda'$, to obtain $\mathcal{E}(u) = \mathcal{E}_{\text{norm}}^{3\text{d}}(y^u)$.

361 Of course we assume that V' is frame-indifferent, $V'(QA) = V'(A)$ for all A
 362 and $Q \in O(3)$. Furthermore, we assume that V' is invariant under relabelling of
 363 atoms (permutation invariance). In particular, this means that V' is compatible with
 364 the lattice symmetries of Λ' : $V'(A) = V'((A_{-\rho})_{\rho \in \Lambda'})$ and $V'(A) = V'((A_{Q'\rho})_{\rho \in \Lambda'})$,
 365 where Q' is the rotation through $2\pi/3$ with axis e_3 . Λ' is also invariant under line
 366 reflection symmetry with respect to the line spanned by $a' = (\frac{\sqrt{3}}{2}, \frac{1}{2}, 0)^T$. Denoting
 367 the reflection map by S' we thus have $V'(A) = V'((A_{S'\rho})_{\rho \in \Lambda'})$.

368 We can now translate these properties to symmetries of V . Clearly, $\mathcal{R} = -\mathcal{R}$ and
 369 $Q_\Lambda \mathcal{R} = \mathcal{R}$. The symmetry properties of V' directly imply $V(A) = V((A_{Q_\Lambda \rho})_{\rho \in \mathcal{R}})$
 370 and $V(A) = V((-A_{-\rho})_{\rho \in \mathcal{R}})$ for all $A \in \mathbb{R}^{\mathcal{R}}$. The slip invariance $V(A) = V(A +$
 371 $p(\delta_{\rho\sigma})_{\sigma \in \mathcal{R}})$ also follows from permutation invariance of V' . We have thus obtained
 372 all the general assumptions that we imposed on V in [Section 2.1](#).

373 Additionally, we will exploit the line reflection symmetry. Let $a = (\frac{\sqrt{3}}{2}, \frac{1}{2})^T$. A
 374 reflection at the line spanned by a in \mathbb{R}^2 is given by

$$375 \quad S = a \otimes a - a^\perp \otimes a^\perp = \begin{pmatrix} \frac{1}{2} & \frac{\sqrt{3}}{2} \\ \frac{\sqrt{3}}{2} & -\frac{1}{2} \end{pmatrix}.$$

376 Due to the line reflection symmetry described by S' as well as frame-indifference with
 377 $Q = S'$, we deduce

$$378 \quad (15) \quad S\mathcal{R} = \mathcal{R}, \quad \text{and} \quad V(A) = V((-A_{S\rho})_{\rho \in \mathcal{R}}).$$

379 We emphasize that Λ' is *not invariant* under a rotation by only $\pi/3$ around the
 380 axis e_3 . This is easily seen, as this rotation maps Λ_2 to Λ_3 and vice versa. Equivalently,
 381 it is not invariant under the mirror symmetry $x \mapsto (x_1, x_2, -x_3)^T$ expressed by [\(9\)](#).
 382 Therefore, the more specific results from the previous section, [Section 2.2](#), do not
 383 apply.

384 While in the setting of [Section 2.2](#) screw dislocations with Burgers vector $b = p$
 385 and $b = -p$ are equivalent, the loss of mirror symmetry in the BCC crystal also
 386 creates two distinctively different screw dislocations, the so-called easy and hard core.
 387 In particular, they have a different core structure; see e.g. [\[13\]](#).

388 The improved decay rates we obtained in [Section 2.2](#) no longer hold up either.
 389 Indeed, one can see in numerical calculations, see [Section 3](#), that the $|x|^{-2}$ bound on
 390 the decay of the strains is sharp (up to logarithmic terms and constants).

391 Our aim now, as announced in the Introduction, is to develop a new far-field
 392 predictor so that the corresponding corrector recovers the higher $|x|^{-4}$ accuracy of
 393 the more symmetric case. A natural first idea is to replace CLE with the Cauchy–
 394 Born nonlinear elasticity equation, however, these are not easy to solve analytically.
 395 Instead, we expand the solution $u = \hat{u} + u_1 + u_2 + \dots$ hoping for $\nabla^j u_2 \ll \nabla^j u_1 \ll \nabla^j \hat{u}$,
 396 which yields

$$397 \quad \begin{aligned} \operatorname{div} \nabla W(\nabla u) &\sim \operatorname{div} \nabla^2 W(0) \nabla \hat{u} \\ 398 \quad &+ \operatorname{div} \left(\nabla^2 W(0) \nabla u_1 + \frac{1}{2} \nabla^3 W(0) [\nabla \hat{u}, \nabla \hat{u}] \right) \\ 399 \quad &+ \operatorname{div} \left(\nabla^2 W(0) \nabla u_2 + \nabla^3 W(0) [\nabla \hat{u}, \nabla u_1] + \nabla^4 W(0) [\nabla \hat{u}, \nabla \hat{u}, \nabla \hat{u}] \right) + \dots \end{aligned}$$

401 The atomistic-continuum error is typically expected to be of comparable size as
 402 the last terms. But, as the projected lattice is still a triangular lattice, many of the

arguments discussed in [Section 2.2](#) still apply and the highest order of this error as well as the term $\nabla^4 W(0)[\nabla \hat{u}, \nabla \hat{u}, \nabla \hat{u}]$ vanish. However, we now have $\nabla^3 W(0) \neq 0$ making the remaining terms non-trivial. We can thus obtain the first two corrections to \hat{u} by solving the linear PDEs

$$(16a) \quad -\operatorname{div} \nabla^2 W(0) \nabla u_1 = \frac{1}{2} \operatorname{div} \left(\nabla^3 W(0) [\nabla \hat{u}, \nabla \hat{u}] \right),$$

$$(16b) \quad -\operatorname{div} \nabla^2 W(0) \nabla u_2 = \operatorname{div} \left(\nabla^3 W(0) [\nabla \hat{u}, \nabla u_1] \right)$$

on $\mathbb{R}^2 \setminus \{0\}$.

Due to [Corollaries 5.4](#) and [5.5](#) below, exploiting the rotational crystalline symmetry, we can simplify them as

$$(17a) \quad -c_{\text{lin}} \Delta u_1 = c_{\text{quad}} \begin{pmatrix} \partial_{11} \hat{u} - \partial_{22} \hat{u} \\ -2\partial_{12} \hat{u} \end{pmatrix} \cdot \nabla \hat{u},$$

$$(17b) \quad -c_{\text{lin}} \Delta u_2 = c_{\text{quad}} \left(\begin{pmatrix} \partial_{11} u_1 - \partial_{22} u_1 \\ -2\partial_{12} u_1 \end{pmatrix} \cdot \nabla \hat{u} + \begin{pmatrix} \partial_{11} \hat{u} - \partial_{22} \hat{u} \\ -2\partial_{12} \hat{u} \end{pmatrix} \cdot \nabla u_1 \right).$$

where

$$c_{\text{lin}} = \frac{1}{2} \operatorname{tr} \nabla^2 W(0), \quad \text{and}$$

$$c_{\text{quad}} = \frac{1}{4} (\nabla^3 W(0)_{111} - 3\nabla^3 W(0)_{122}).$$

~~420~~

In polar coordinates, $x = \hat{x} + r(\cos \varphi, \sin \varphi)^T$, using the fact that $\hat{u} = \frac{b}{2\pi} \arg(x - \hat{x}) = \frac{b}{2\pi} \varphi$, [Eq. \(17a\)](#) becomes

$$-\Delta u_1 = \frac{c_{\text{quad}} b^2 \cos(3\varphi)}{c_{\text{lin}} 2\pi^2 r^3},$$

from which we readily infer that one possible solution is

$$(18) \quad u_1(x + \hat{x}) = \frac{c_{\text{quad}} b^2 \cos(3\varphi)}{c_{\text{lin}} 16\pi^2 r} = \frac{c_{\text{quad}} b^2}{c_{\text{lin}} 16\pi^2} \frac{x_1^3 - 3x_1 x_2^2}{|x|^4}.$$

Similarly, inserting \hat{u} and u_1 into [Eq. \(17b\)](#) yields

$$-\Delta u_2 = \frac{c_{\text{quad}}^2 b^3 \sin(6\varphi)}{c_{\text{lin}}^2 4\pi^3 r^4},$$

for which a solution is given by

$$(19) \quad u_2(x + \hat{x}) = \frac{c_{\text{quad}}^2 b^3 \sin(6\varphi)}{c_{\text{lin}}^2 128\pi^3 r^2} = \frac{c_{\text{quad}}^2 b^3}{c_{\text{lin}}^2 128\pi^3} \frac{6x_1^5 x_2 - 20x_1^3 x_2^3 + 6x_1 x_2^5}{|x|^8}.$$

While there are many more solutions for both problems, we will choose these specific ones as they satisfy the decay estimates

$$(20) \quad |\nabla^j u_i| \lesssim |x|^{-i-j}$$

and the rotational symmetry $u_i(L_Q x) = u_i(x)$. With the solutions u_1 and u_2 obtained, respectively, in [\(18\)](#) and [\(19\)](#) we obtain the following result.

435 **THEOREM 2.9 (BCC).** *Let $\Lambda = A_{\text{tri}}\mathbb{Z}^2$ and suppose $\Lambda, \hat{x}, \mathcal{R}, V$ satisfy all the as-*
 436 *sumptions from [Section 2.1](#). Furthermore, assume \mathcal{R} and V satisfy the line reflection*
 437 *symmetry [\(15\)](#). Consider a critical point \bar{u} of [\(1\)](#) that inherits the rotational symme-*
 438 *try of \hat{u} . Then we can write $\bar{u} = u_1 + u_2 + \bar{u}_{\text{rem}}$ where u_1 and u_2 are given by [\(18\)](#)*
 439 *and [\(19\)](#) and the remainder \bar{u}_{rem} satisfies the decay estimates*

$$440 \quad (21) \quad |D^j \bar{u}_{\text{rem}}(x)| \lesssim |x|^{-j-3} \log|x|,$$

441 *for $j = 1, 2$ and all $|x|$ large enough.*

442 *Remark 2.10.* As discussed in the introduction, our new predictor $\hat{u} + u_1 + u_2$
 443 does not just result in $O(|x|^{-3})$ accuracy for the strain which one might expect from
 444 the general expansion idea or from well-established results about the Cauchy-Born
 445 anti-discretisation error. The actual accuracy is one order higher, i.e., $O(|x|^{-4})$.

446 *Remark 2.11.* Since $|D^j u_1(x)| \lesssim |x|^{-j-1}$, without log-factors, [Theorem 2.9](#) im-
 447 proves the result of [Theorem 2.2](#) to

$$448 \quad |D^j \bar{u}(x)| \lesssim |x|^{-j-1}, \quad j = 1, 2.$$

449 **3. Numerical approximation.**

450 **3.1. Supercell approximation.** A central motivation for the present work are
 451 the poor convergence rates of standard supercell approximations for the defect equi-
 452 libration problem [\(8\)](#) established in [\[8\]](#). We can now exploit the theoretical results
 453 from [Section 2](#) to construct boundary conditions that give rise to new supercell ap-
 454 proximations. These have improved rates of convergence without any corresponding
 455 increase in computational complexity.

456 We begin by defining a generalised energy-difference functional in a predictor-
 457 corrector form

$$458 \quad \mathcal{E}(u_{\text{pred}}; u) := \sum_{x \in \Lambda} V(Du_{\text{pred}}(x) + Du(x)) - V(Du_{\text{pred}}(x)),$$

$$459 \quad \text{for } u_{\text{pred}} \in \hat{u} + \dot{\mathcal{H}}^1, u \in \dot{\mathcal{H}}^1.$$

461 Then, the generalised variational problem

$$462 \quad (22) \quad \tilde{u} \in \arg \min \{ \mathcal{E}(u_{\text{pred}}; u) \mid u \in \dot{\mathcal{H}}^1 \}$$

463 is equivalent to [\(8\)](#), via the identity $u_{\text{pred}} + \tilde{u} = \hat{u} + \bar{u}$.

464 We now note as in [\[8\]](#) that the supercell approximation on a domain $B_R \cap \Lambda \subset$
 465 $\Omega_R \subset \Lambda$ with boundary condition u_{pred} on $\Lambda \setminus \Omega_R$ can be written as a Galerkin
 466 approximation

$$467 \quad (23) \quad \tilde{u}_R \in \arg \min \{ \mathcal{E}(u_{\text{pred}}; u) \mid u \in \mathcal{H}^0(\Omega_R) \},$$

$$468 \quad \text{where } \mathcal{H}^0(\Omega_R) := \{ v \in \mathcal{H}^c \mid v = 0 \text{ in } \Lambda \setminus \Omega_R \}.$$

470 Using generic properties of Galerkin approximations we obtain the following ap-
 471 proximation error estimate.

472 **THEOREM 3.1.** *Let \tilde{u} be a strongly stable solution (cf. [\[8\]](#)) to [\(22\)](#), i.e. satisfying*

$$473 \quad \delta_u^2 \mathcal{E}(u_{\text{pred}}; \tilde{u})[v, v] \geq \lambda \|v\|_{\dot{\mathcal{H}}^1}^2,$$

474 for all $v \in \mathcal{H}^c$ and a $\lambda > 0$. If \tilde{u} further satisfies

$$475 \quad |D\tilde{u}(x)| \lesssim |x|^{-s} \log^r |x|,$$

476 for some $s > 1, r \in \{0, 1\}$, then there exist $C, R_0 > 0$ such that, for all $R > R_0$ there
 477 exists a stable solution \tilde{u}_R to (23) satisfying

$$478 \quad (24) \quad \|\tilde{u}_R - \tilde{u}\|_{\dot{\mathcal{H}}^1} \leq CR^{-s+1} \log^r(R).$$

479 *Proof.* The existence of a solution \tilde{u}_R , for R sufficiently large, can be proven as in
 480 [7, Theorem 2.4] (the case $u_{\text{pred}} = \hat{u}$) and the equivalence of (22) with (8). Moreover,
 481 following the proof of [8, Theorem 6] verbatim we obtain

$$482 \quad \|\tilde{u}_R - \tilde{u}\|_{\dot{\mathcal{H}}^1} \lesssim \|\tilde{u}\|_{\dot{\mathcal{H}}^1(\Lambda \setminus B_{R/2})}.$$

484 We then apply the assumption that $|D\tilde{u}(x)| \lesssim |x|^{-s} \log^r |x|$ to arrive at the desired
 485 error estimate,

$$\|\tilde{u}_R - \tilde{u}\|_{\dot{\mathcal{H}}^1} \lesssim \left(\sum_{x \in \Lambda \setminus B_{R/2}} |D\tilde{u}(x)|^2 \right)^{1/2} \lesssim \left(\int_{\frac{R}{3}}^{\infty} t^{1-2s} \log^{2r}(t) dt \right)^{\frac{1}{2}} \lesssim R^{1-s} \log^r(R).$$

486

□

487 **3.2. Numerical examples with mirror symmetry.** To test the results from
 488 Section 2.2 we consider a toy model involving nearest-neighbour pair interaction,

$$489 \quad V(Du(x)) = \sum_{\rho \in \mathcal{R}} \psi(D_\rho u(x)), \quad \psi(r) = \sin^2(\pi r),$$

490 which is 1-periodic, i.e., $p = 1$. We investigate the three cases

491 (i) symmetric square:

$$492 \quad \Lambda = \mathbb{Z}^2, \quad \mathcal{R} = \{\pm e_1, \pm e_2\}, \quad \hat{x} = \begin{pmatrix} \frac{1}{2} \\ \frac{1}{2} \end{pmatrix};$$

493 (ii) symmetric triangular:

$$494 \quad \Lambda = A_{\text{tri}}\mathbb{Z}^2, \quad \mathcal{R} = \left\{ \pm \begin{pmatrix} 1 \\ 0 \end{pmatrix}, \pm \begin{pmatrix} \frac{1}{2} \\ \frac{\sqrt{3}}{2} \end{pmatrix}, \pm \begin{pmatrix} -\frac{1}{2} \\ \frac{\sqrt{3}}{2} \end{pmatrix} \right\}, \quad \hat{x} = \begin{pmatrix} \frac{1}{2} \\ \frac{\sqrt{3}}{6} \end{pmatrix};$$

495 (iii) asymmetric triangular: as in (ii), but with $\hat{x} = \begin{pmatrix} \frac{1}{4} \\ \frac{1}{8} \end{pmatrix}$.

496 The cases (i) and (ii) satisfy all conditions of Theorem 2.5 while (iii) fails the crucial
 497 symmetry assumptions. In particular, at least up to logarithmic terms, our theory
 498 predicts $|D\bar{u}(x)| \lesssim |x|^{-3}$ for (i), $|D\bar{u}(x)| \lesssim |x|^{-4}$ for (ii), and $|D\bar{u}(x)| \lesssim |x|^{-2}$ for (iii).
 499 Due to Theorem 3.1 this corresponds to $\|\tilde{u}_R - \tilde{u}\|_{\dot{\mathcal{H}}^1}$ being $O(R^{-2})$, $O(R^{-3})$, and
 500 $O(R^{-1})$, respectively. To compute equilibria we employ a standard Newton scheme,
 501 terminated at an ℓ^∞ -residual of 10^{-8} . In Figure 2 we plot both the decay of the
 502 correctors, confirming the predictions of Theorem 2.5, and the approximation error
 503 in the supercell approximation against the domain size R , confirming the prediction
 504 of Theorem 3.1.

505 *Remark 3.2.* An asymmetric square case (that is as in (i) but with $\hat{x} = (\frac{1}{3}, \frac{1}{3})$)
 506 has also been considered and the results are as expected by our theory and thus are
 507 qualitatively equivalent to (iii). Therefore we do not include them in the figures to
 508 retain clarity. It does however further emphasise the role of symmetry in the problem.

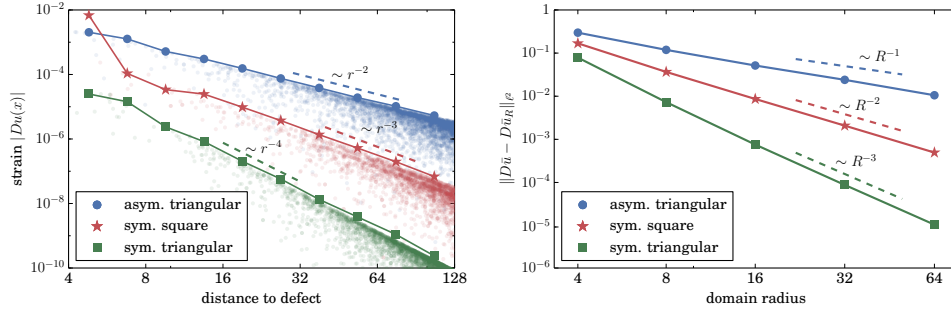


FIG. 2. Left: Decay of $|D\bar{u}|$ for the square and triangular lattices, with and without rotational symmetry. Transparent dots denote data points $(|x|, |Du(x)|)$, solid curves their envelopes. We observe the improved decay rates r^{-3} and r^{-4} , proven in [Theorem 2.5](#), when the dislocation core is chosen as a high symmetry point.

Right: Rates of convergence of the supercell approximation (23) in the three cases specified in [Section 3.2](#). We observe the improved rates of convergence in the high symmetry cases as predicted by [Theorem 3.1](#).

509 **3.3. Numerical example in BCC Tungsten.** To confirm the result of [Section](#)
 510 [2.3](#), we consider a Finnis–Sinclair type model (EAM model) for BCC Tungsten
 511 (W), where the 3D site energy for a deformation y is of the form

$$512 \quad V'(D'y) = -\left(\sum_{\sigma \in \Lambda'} \rho(|D_\sigma y|)\right)^{1/2} + \sum_{\sigma \in \Lambda'} \phi(|D_\sigma y|),$$

513 and the electron density ρ and pair repulsion ϕ are obtained from [\[19\]](#). The pro-
 514 jected anti-plane model is then constructed as described in [Section 2.3](#). The supercell
 515 model (23) is solved to within an ℓ^∞ residual of 10^{-6} using a preconditioned LBFGBS
 516 algorithm [\[17\]](#).

517 We investigate two test cases, the easy dislocation core (negatively oriented) and
 518 the hard dislocation core (positively oriented), cf. [\[13\]](#). For each case, following
 519 [Section 2.3](#), we consider three different predictors:

- 520 (i) standard linearised elasticity predictor (0th order), i.e., $u_{\text{pred}} = \hat{u}$;
- 521 (ii) 1st order correction, i.e. $u_{\text{pred}} = \hat{u} + u_1$;
- 522 (iii) 2nd order correction, i.e. $u_{\text{pred}} = \hat{u} + u_1 + u_2$,

523 with \hat{u} given in [\(7\)](#) and u_1, u_2 , respectively, in [\(18\)](#) and [\(19\)](#).

524 In [Figures 3](#) and [4](#) on the left-hand side we display the decay of the correctors for,
 525 respectively, the hard (positive) and easy (negative) dislocation cores, confirming the
 526 prediction of [Theorem 2.9](#). On the right-hand side we plot the corresponding approx-
 527 imation errors in the supercell approximation against the domain size R , confirming
 528 the prediction of [Theorem 3.1](#).

529 **4. Conclusion.** We have developed a range of results establishing finer proper-
 530 ties of the elastic far-field generated by a screw dislocation in anti-plane shear kine-
 531 matics. Of particular note is the role that crystalline symmetries play in obtaining
 532 either cancellation (screw and square lattice) or simple and explicit representations
 533 of the leading order terms of this elastic far-field. As a key application we showed
 534 how these results can be exploited to obtain boundary conditions with significantly
 535 improved convergence rates in terms of computational cell size.

536 Crucial to these results is the idea that solutions inherit the symmetries from the
 537 setting of the problem. While the validity of this assumption is likely very difficult to

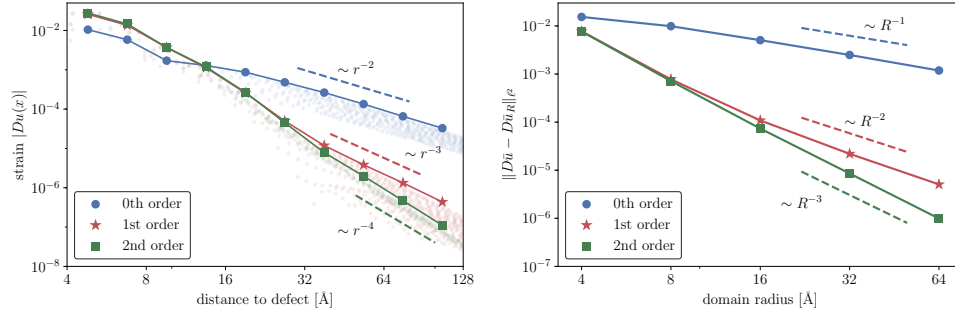


FIG. 3. *Left: Decay of $|D\bar{u}|$ for a BCC easy core screw dislocation with standard and improved far-field predictors; cf. Section 3.3. Transparent dots denote data points $(|x|, |Du(x)|)$, solid curves their envelopes. The numerically observed improved decay for higher-order predictors is consistent with Theorem 2.9.*

Right: Rates of convergence of the supercell approximation (23) to the BCC easy core screw dislocation, employing the standard as well as higher-order far-field predictors. The improved rates of convergence due to the faster decay of the corrector solutions are consistent with Theorem 3.1.

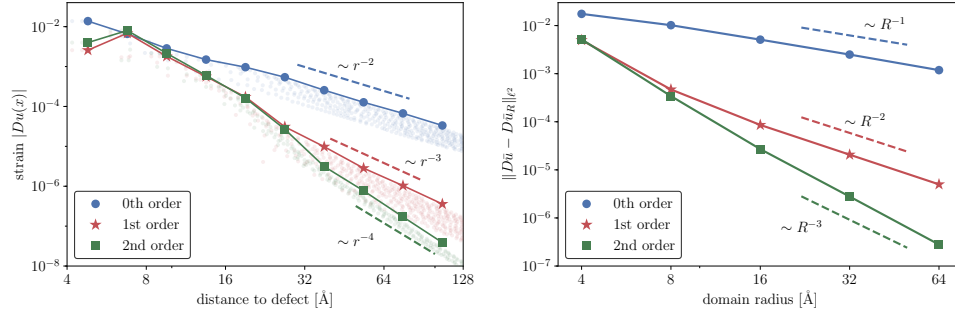


FIG. 4. *Left: Decay of $|D\bar{u}|$ for a BCC hard core screw dislocation with standard and improved far-field predictors; cf. Section 3.3. Transparent dots denote data points $(|x|, |Du(x)|)$, solid curves their envelopes. The numerically observed improved decay for higher-order predictors is consistent with Theorem 2.9.*

Right: Rates of convergence of the supercell approximation (23) to the BCC hard core screw dislocation, employing the standard as well as higher-order far-field predictors. The improved rates of convergence due to the faster decay of the corrector solutions are consistent with Theorem 3.1.

538 be proven without prohibitively restrictive assumptions on the interatomic interaction,
 539 our numerical tests, show-casing the improved rates of decay of the core correctors
 540 and resulting improved convergence rates, indicate that in these cases the inheritance
 541 of symmetry is indeed reasonable. In particular, our results clearly explain the origin
 542 of these improved rates.

543 The general ideas that we outlined in this paper set the scene for an in-depth
 544 study of the elastic far-field for a large variety of defect types, fully vectorial models,
 545 and more general crystalline solids. The resulting derivation of higher-order boundary
 546 conditions promises to yield simple, efficient as well as highly accurate new algorithms
 547 to simulate crystalline defects.

548 5. Proofs.

549 **5.1. Auxiliary results about symmetry.** We prove the main results through
 550 a number of lemmas, starting with the following observations about how symmetry
 551 simplifies the tensors appearing in the development of the forces. This includes, but

552 is not limited to the tensors $\nabla^2 W(0) \in \mathbb{R}^{2 \times 2} = (\mathbb{R}^2)^{\otimes 2}$, $\nabla^3 W(0) \in (\mathbb{R}^2)^{\otimes 3}$, and
 553 $\nabla^4 W(0) \in (\mathbb{R}^2)^{\otimes 4}$.

554 Let $m \in \mathbb{N}$, $A \in (\mathbb{R}^2)^{\otimes m}$ and $B \in \mathbb{R}^{2 \times 2}$ then the tensor $B^{\otimes m} A \in (\mathbb{R}^2)^{\otimes m}$ is, as
 555 usual, defined by

$$556 \quad (B^{\otimes m} A)_{l_1 \dots l_m} := \sum_{k \in \{1,2\}^m} A_{k_1 \dots k_m} \prod_{i=1}^m B_{l_i k_i}.$$

557 As before let Q be a matrix representing either a rotation by $\pi/2$ (in the case $\Lambda = \mathbb{Z}^2$)
 558 or a rotation by $2\pi/3$ (in the case $\Lambda = A_{\text{tri}} \mathbb{Z}^2$). That is,

$$559 \quad Q = \begin{pmatrix} 0 & -1 \\ 1 & 0 \end{pmatrix} \text{ or } Q = \begin{pmatrix} -\frac{1}{2} & -\frac{\sqrt{3}}{2} \\ \frac{\sqrt{3}}{2} & -\frac{1}{2} \end{pmatrix}.$$

560 More generally, let $Q \in \mathbb{R}^{2 \times 2}$ with $Q^N = \text{Id}$ for some $N \in \mathbb{N}$, $N \geq 1$, and $Q^T Q = \text{Id}$.
 561 Our specific cases are included as $N = 4$ and $N = 3$. We then define

$$562 \quad PA = \frac{1}{N} \sum_{M=0}^{N-1} (Q^M)^{\otimes m} A.$$

563 Consider the standard scalar product for tensors,

$$564 \quad A : B = \sum_{k_1, \dots, k_m=1}^2 A_{k_1 \dots k_m} B_{k_1 \dots k_m}.$$

565 Then we have the following lemma.

566 LEMMA 5.1. *P is the orthogonal projector onto the Q-invariant tensors*

$$567 \quad \{A : Q^{\otimes m} A = A\}.$$

568 *Proof.* One readily checks that $Q^{\otimes m}((Q^M)^{\otimes m} A) = (Q^{M+1})^{\otimes m} A$. Using also
 569 $Q^N = \text{Id}$ one immediately obtains $Q^{\otimes m} P A = P A$. Therefore, $P^2 = P$. Since
 570 $(Q^M)^T = Q^{-M} = Q^{N-M}$, we also see that P is self-adjoint. Hence, P is an orthogonal
 571 projection onto a subspace of $\{A : Q^{\otimes m} A = A\}$. But if $Q^{\otimes m} A = A$ then clearly
 572 $P A = A$, which concludes the proof. \square

573 Lemma 5.1 will prove highly useful: Explicitly calculating P now allows us to
 574 characterise the rotationally invariant tensors.

575 To simplify that calculation further, we also define the symmetric part by

$$576 \quad (\text{sym } A)_{l_1 \dots l_m} = \frac{1}{m!} \sum_{\varphi \in S_m} A_{\varphi(l_1) \dots \varphi(l_m)},$$

577 where S_m is the group of all permutations on m numbers. For all A we define

$$578 \quad P_{\text{sym}} A := P \text{sym } A = \text{sym } P A.$$

579 Let us calculate these projections and thus the invariant spaces for the cases we
 580 encounter in our proof later.

581 For a simple notation of three-tensors and four-tensors in the following we will
 582 write $E_{ijk} = e_i \otimes e_j \otimes e_k$ and $E_{ijkl} = e_i \otimes e_j \otimes e_k \otimes e_l$ where $\{e_1, e_2\}$ represents the
 583 standard base of \mathbb{R}^2 .

584 LEMMA 5.2. (a) For $m = 2$ and $N \geq 3$,

$$585 \quad P_{\text{sym}}A = \frac{1}{2} \text{tr}(A) \text{Id}, \quad i.e., \quad \{A: Q^{\otimes 2}A = A, \text{sym } A = A\} = \text{span Id}.$$

586 (b) For $m = 3$ and $N = 3$,

$$587 \quad P_{\text{sym}}A = \frac{1}{4}(E_{111} - 3 \text{sym } E_{122})(A_{111} - 3 \text{sym } A_{122}) \\ 588 \quad + \frac{1}{4}(E_{222} - 3 \text{sym } E_{112})(A_{222} - 3 \text{sym } A_{112}), \\ 589 \quad i.e., \{A: Q^{\otimes 3}A = A, \text{sym } A = A\} = \text{span}\{E_{111} - 3 \text{sym } E_{122}, E_{222} - 3 \text{sym } E_{112}\}.$$

591 (c) For $m = 4$ and $N = 3$,

$$592 \quad (P_{\text{sym}}A)_{abcd} = \frac{1}{8}(\delta_{ab}\delta_{cd} + \delta_{ac}\delta_{bd} + \delta_{ad}\delta_{bc})(A_{1111} + 2 \text{sym } A_{1122} + A_{2222}), \\ 593 \quad i.e., \{A: Q^{\otimes 4}A = A, \text{sym } A = A\} = \text{span}\{E_{1111} + E_{2222} + 2 \text{sym } E_{1122}\}.$$

595 *Proof.* (a) We have $(Q \otimes Q)A = A$ if and only if $QAQ^T = A$. For symmetric A ,
596 we can diagonalize $A = RDR^T$ with some rotation R and a diagonal matrix D . But
597 then $QAQ^T = A$ is equivalent to $QDQ^T = D$. This is the case precisely if $D = c \text{Id}$ or
598 $Q \in \{\pm \text{Id}\}$. Since we excluded the latter option we find $\{A: (Q \otimes Q)A = A\} = \text{Id } \mathbb{R}$
599 as claimed.

600 (b) This statement is more involved and notably depends on N . Therefore a general
601 argument as in (a) cannot work. One way of obtaining the result is to calculate the
602 projector explicitly. By linearity, it suffices to consider $A = \sigma \otimes \rho \otimes \tau$. In this case,
603 $Q^{\otimes m}A = Q\sigma \otimes Q\rho \otimes Q\tau$. We get

$$604 \quad 3(P(\sigma \otimes \rho \otimes \tau))_{111} = \sigma_1\rho_1\tau_1 + (-\frac{1}{2}\sigma_1 - \frac{\sqrt{3}}{2}\sigma_2)(-\frac{1}{2}\rho_1 - \frac{\sqrt{3}}{2}\rho_2)(-\frac{1}{2}\tau_1 - \frac{\sqrt{3}}{2}\tau_2) \\ 605 \quad + (-\frac{1}{2}\sigma_1 + \frac{\sqrt{3}}{2}\sigma_2)(-\frac{1}{2}\rho_1 + \frac{\sqrt{3}}{2}\rho_2)(-\frac{1}{2}\tau_1 + \frac{\sqrt{3}}{2}\tau_2) \\ 606 \quad = \frac{3}{4}(\sigma_1\rho_1\tau_1 - \sigma_1\rho_2\tau_2 - \sigma_2\rho_1\tau_2 - \sigma_2\rho_2\tau_1), \\ 607 \quad 3(P(\sigma \otimes \rho \otimes \tau))_{222} = \sigma_2\rho_2\tau_2 + (\frac{\sqrt{3}}{2}\sigma_1 - \frac{1}{2}\sigma_2)(\frac{\sqrt{3}}{2}\rho_1 - \frac{1}{2}\rho_2)(\frac{\sqrt{3}}{2}\tau_1 - \frac{1}{2}\tau_2) \\ 608 \quad + (-\frac{\sqrt{3}}{2}\sigma_1 - \frac{1}{2}\sigma_2)(-\frac{\sqrt{3}}{2}\rho_1 - \frac{1}{2}\rho_2)(-\frac{\sqrt{3}}{2}\tau_1 - \frac{1}{2}\tau_2) \\ 609 \quad = \frac{3}{4}(\sigma_2\rho_2\tau_2 - \sigma_1\rho_1\tau_2 - \sigma_1\rho_2\tau_1 - \sigma_2\rho_1\tau_1), \\ 610 \quad 3(P(\sigma \otimes \rho \otimes \tau))_{112} = \sigma_1\rho_1\tau_2 + (-\frac{1}{2}\sigma_1 - \frac{\sqrt{3}}{2}\sigma_2)(-\frac{1}{2}\rho_1 - \frac{\sqrt{3}}{2}\rho_2)(\frac{\sqrt{3}}{2}\tau_1 - \frac{1}{2}\tau_2) \\ 611 \quad + (-\frac{1}{2}\sigma_1 + \frac{\sqrt{3}}{2}\sigma_2)(-\frac{1}{2}\rho_1 + \frac{\sqrt{3}}{2}\rho_2)(-\frac{\sqrt{3}}{2}\tau_1 - \frac{1}{2}\tau_2) \\ 612 \quad = \frac{3}{4}(-\sigma_2\rho_2\tau_2 + \sigma_1\rho_1\tau_2 + \sigma_1\rho_2\tau_1 + \sigma_2\rho_1\tau_1), \quad \text{and} \\ 613 \quad 3(P(\sigma \otimes \rho \otimes \tau))_{122} = \sigma_1\rho_2\tau_2 + (-\frac{1}{2}\sigma_1 - \frac{\sqrt{3}}{2}\sigma_2)(\frac{\sqrt{3}}{2}\rho_1 - \frac{1}{2}\rho_2)(\frac{\sqrt{3}}{2}\tau_1 - \frac{1}{2}\tau_2) \\ 614 \quad + (-\frac{1}{2}\sigma_1 + \frac{\sqrt{3}}{2}\sigma_2)(-\frac{\sqrt{3}}{2}\rho_1 - \frac{1}{2}\rho_2)(-\frac{\sqrt{3}}{2}\tau_1 - \frac{1}{2}\tau_2) \\ 615 \quad = \frac{3}{4}(-\sigma_1\rho_1\tau_1 + \sigma_1\rho_2\tau_2 + \sigma_2\rho_1\tau_2 + \sigma_2\rho_2\tau_1).$$

617 This concludes (b).

618 (c) Again, this statement depends on N , so we will calculate the projector explicitly.

619 Similar as before, it suffices to consider $A = \pi \otimes \sigma \otimes \rho \otimes \tau$. We find

$$\begin{aligned}
620 \quad 3(PA)_{1111} &= \pi_1 \sigma_1 \rho_1 \tau_1 \\
621 \quad &+ \left(-\frac{1}{2}\pi_1 - \frac{\sqrt{3}}{2}\pi_2\right) \left(-\frac{1}{2}\sigma_1 - \frac{\sqrt{3}}{2}\sigma_2\right) \left(-\frac{1}{2}\rho_1 - \frac{\sqrt{3}}{2}\rho_2\right) \left(-\frac{1}{2}\tau_1 - \frac{\sqrt{3}}{2}\tau_2\right) \\
622 \quad &+ \left(-\frac{1}{2}\pi_1 + \frac{\sqrt{3}}{2}\pi_2\right) \left(-\frac{1}{2}\sigma_1 + \frac{\sqrt{3}}{2}\sigma_2\right) \left(-\frac{1}{2}\rho_1 + \frac{\sqrt{3}}{2}\rho_2\right) \left(-\frac{1}{2}\tau_1 + \frac{\sqrt{3}}{2}\tau_2\right) \\
623 \quad &= \frac{9}{8}(\pi_1 \sigma_1 \rho_1 \tau_1 + \pi_2 \sigma_2 \rho_2 \tau_2) + \frac{3}{8}(\pi_1 \sigma_1 \rho_2 \tau_2 + \pi_1 \sigma_2 \rho_1 \tau_2 \\
624 \quad &+ \pi_1 \sigma_2 \rho_2 \tau_1 + \pi_2 \sigma_1 \rho_1 \tau_2 + \pi_2 \sigma_1 \rho_2 \tau_1 + \pi_2 \sigma_2 \rho_1 \tau_1) \quad \text{and} \\
625 \quad 3(PA)_{2222} &= \pi_2 \sigma_2 \rho_2 \tau_2 \\
626 \quad &+ \left(\frac{\sqrt{3}}{2}\pi_1 - \frac{1}{2}\pi_2\right) \left(\frac{\sqrt{3}}{2}\sigma_1 - \frac{1}{2}\sigma_2\right) \left(\frac{\sqrt{3}}{2}\rho_1 - \frac{1}{2}\rho_2\right) \left(\frac{\sqrt{3}}{2}\tau_1 - \frac{1}{2}\tau_2\right) \\
627 \quad &+ \left(-\frac{\sqrt{3}}{2}\pi_1 - \frac{1}{2}\pi_2\right) \left(-\frac{\sqrt{3}}{2}\sigma_1 - \frac{1}{2}\sigma_2\right) \left(-\frac{\sqrt{3}}{2}\rho_1 - \frac{1}{2}\rho_2\right) \left(-\frac{\sqrt{3}}{2}\tau_1 - \frac{1}{2}\tau_2\right) \\
628 \quad &= \frac{9}{8}(\pi_1 \sigma_1 \rho_1 \tau_1 + \pi_2 \sigma_2 \rho_2 \tau_2) + \frac{3}{8}(\pi_1 \sigma_1 \rho_2 \tau_2 + \pi_1 \sigma_2 \rho_1 \tau_2 \\
629 \quad &+ \pi_1 \sigma_2 \rho_2 \tau_1 + \pi_2 \sigma_1 \rho_1 \tau_2 + \pi_2 \sigma_1 \rho_2 \tau_1 + \pi_2 \sigma_2 \rho_1 \tau_1).
\end{aligned}$$

631 By interchanging π, σ, ρ, τ , the even mixed terms can be reduced to calculating just

$$\begin{aligned}
632 \quad 3(PA)_{1122} &= \pi_1 \sigma_1 \rho_2 \tau_2 \\
633 \quad &+ \left(-\frac{1}{2}\pi_1 - \frac{\sqrt{3}}{2}\pi_2\right) \left(-\frac{1}{2}\sigma_1 - \frac{\sqrt{3}}{2}\sigma_2\right) \left(\frac{\sqrt{3}}{2}\rho_1 - \frac{1}{2}\rho_2\right) \left(\frac{\sqrt{3}}{2}\tau_1 - \frac{1}{2}\tau_2\right) \\
634 \quad &+ \left(-\frac{1}{2}\pi_1 + \frac{\sqrt{3}}{2}\pi_2\right) \left(-\frac{1}{2}\sigma_1 + \frac{\sqrt{3}}{2}\sigma_2\right) \left(-\frac{\sqrt{3}}{2}\rho_1 - \frac{1}{2}\rho_2\right) \left(-\frac{\sqrt{3}}{2}\tau_1 - \frac{1}{2}\tau_2\right) \\
635 \quad &= \frac{9}{8}(\pi_1 \sigma_1 \rho_2 \tau_2 + \pi_2 \sigma_2 \rho_1 \tau_1) + \frac{3}{8}(\pi_1 \sigma_1 \rho_1 \tau_1 + \pi_2 \sigma_2 \rho_2 \tau_2 \\
636 \quad &- \pi_1 \sigma_2 \rho_2 \tau_1 - \pi_2 \sigma_1 \rho_1 \tau_2 - \pi_2 \sigma_1 \rho_2 \tau_1 - \pi_1 \sigma_2 \rho_1 \tau_2).
\end{aligned}$$

638 For the symmetric part, these formulae simplify to

$$\begin{aligned}
639 \quad (P \operatorname{sym} A)_{1111} &= (P \operatorname{sym} A)_{2222} \\
640 \quad &= 3(P \operatorname{sym} A)_{1122} \\
641 \quad &= \frac{3}{8}(\pi_1 \sigma_1 \rho_1 \tau_1 + \pi_2 \sigma_2 \rho_2 \tau_2) + \frac{6}{8} \operatorname{sym}(\pi \otimes \sigma \otimes \rho \otimes \tau)_{1122},
\end{aligned}$$

643 Furthermore,

$$\begin{aligned}
644 \quad 3(PA)_{1112} &= \pi_1 \sigma_1 \rho_1 \tau_2 \\
645 \quad &+ \left(-\frac{1}{2}\pi_1 - \frac{\sqrt{3}}{2}\pi_2\right) \left(-\frac{1}{2}\sigma_1 - \frac{\sqrt{3}}{2}\sigma_2\right) \left(-\frac{1}{2}\rho_1 - \frac{\sqrt{3}}{2}\rho_2\right) \left(\frac{\sqrt{3}}{2}\tau_1 - \frac{1}{2}\tau_2\right) \\
646 \quad &+ \left(-\frac{1}{2}\pi_1 + \frac{\sqrt{3}}{2}\pi_2\right) \left(-\frac{1}{2}\sigma_1 + \frac{\sqrt{3}}{2}\sigma_2\right) \left(-\frac{1}{2}\rho_1 + \frac{\sqrt{3}}{2}\rho_2\right) \left(-\frac{\sqrt{3}}{2}\tau_1 - \frac{1}{2}\tau_2\right) \\
647 \quad &= \frac{9}{8}(\pi_1 \sigma_1 \rho_1 \tau_2 - \pi_2 \sigma_2 \rho_2 \tau_1) + \frac{3}{8}(\pi_2 \sigma_2 \rho_1 \tau_2 + \pi_2 \sigma_1 \rho_2 \tau_2 \\
648 \quad &+ \pi_1 \sigma_2 \rho_2 \tau_2 - \pi_1 \sigma_1 \rho_2 \tau_1 - \pi_2 \sigma_1 \rho_1 \tau_1 - \pi_2 \sigma_1 \rho_1 \tau_1),
\end{aligned}$$

650 which implies $(P \operatorname{sym} A)_{1112} = 0$. In the same spirit one finds $(P \operatorname{sym} A)_{1222} = 0$. \square

651 Additionally, the result for $m = N = 3$ simplifies further if we add line reflection
652 symmetry. As in [Section 2.3](#), let $a = \left(\frac{\sqrt{3}}{2}, \frac{1}{2}\right)^T$ and

$$653 \quad S = a \otimes a - a^\perp \otimes a^\perp = \begin{pmatrix} \frac{1}{2} & \frac{\sqrt{3}}{2} \\ \frac{\sqrt{3}}{2} & -\frac{1}{2} \end{pmatrix}.$$

654 LEMMA 5.3. *For $m = 3$ and $N = 3$ one has*

$$655 \quad \{A: Q^{\otimes 3} A = A, \operatorname{sym} A = A, S^{\otimes 3} A = -A\} = \operatorname{span}\{E_{111} - 3 \operatorname{sym} E_{122}\}.$$

656 *Proof.* Let A be a tensor with $Q^{\otimes 3}A = A$, $\text{sym } A = A$, and $S^{\otimes 3}A = -A$. Ac-
 657 cording to Lemma 5.2, $A = c_1(E_{111} - 3\text{sym } E_{122}) + c_2(E_{222} - 3\text{sym } E_{112})$. Addi-
 658 tionally, $S^{\otimes 3}A = -A$ implies $A[Sa, Sa, Sa] = -A[a, a, a]$. But with $Sa = a$ we have
 659 $A[a, a, a] = 0$; that is,

$$660 \quad 0 = c_1\left(\frac{3\sqrt{3}}{8} - 3\frac{\sqrt{3}}{8}\right) + c_2\left(\frac{1}{8} - 3\frac{3}{8}\right),$$

661 which implies $c_2 = 0$. With the same calculation one also sees the reverse, i.e., that
 662 $E_{222} - 3\text{sym } E_{112}$ does indeed satisfy the reflection symmetry. \square

663 Among other applications later on in the analysis, Lemmas 5.2 and 5.3 can be
 664 used for the following two corollaries. As a first corollary, we recover a classical
 665 result about isotropic linear elasticity (compare, e.g., [14] for the analogous three-
 666 dimensional case).

667 COROLLARY 5.4. *In the setting of Section 2.1, for W given by (5), one finds*
 668 $\nabla^2 W(0) = c_{\text{lin}} \text{Id}$, for some $c_{\text{lin}} > 0$, and therefore

$$669 \quad -\text{div}(\nabla^2 W(0)[\nabla u]) = -c_{\text{lin}} \Delta u$$

670 *Proof.* According to (5) $W(F) = \frac{1}{\det A_\Lambda} V(F \cdot \mathcal{R})$, hence we have

$$671 \quad \nabla^2 W(0) = \frac{1}{\det A_\Lambda} \sum_{\rho, \sigma \in \mathcal{R}} \nabla^2 V(0)_{\rho\sigma\rho} \otimes \sigma.$$

672 We further notice that due to the rotational symmetry of \mathcal{R} and V , (2), we have
 673 $\nabla^2 V(0)_{\rho\sigma} = \nabla^2 V(0)_{Q\rho Q\sigma}$, hence we can equivalently write

$$674 \quad \nabla^2 W(0) = \frac{1}{\det A_\Lambda} \sum_{\rho, \sigma \in \mathcal{R}} \nabla^2 V(0)_{\rho\sigma} Q\rho \otimes Q\sigma.$$

675 In particular,

$$676 \quad \nabla^2 W(0) \in \{A \in \mathbb{R}^{2 \times 2} : (Q \otimes Q)A = A\}.$$

677 It is also clear that $\nabla^2 W(0)$ is symmetric, thus

$$678 \quad P_{\text{sym}} \nabla^2 W(0) = \nabla^2 W(0)$$

679 and so we invoke Lemma 5.2 to conclude that

$$680 \quad \nabla^2 W(0) = \left(\frac{1}{2 \det A_\Lambda} \sum_{\rho, \sigma \in \mathcal{R}} \nabla^2 V(0)_{\rho\sigma\rho} \cdot \sigma \right) \text{Id} =: c_{\text{lin}} \text{Id}.$$

681 Since lattice stability implies Legendre-Hadamard stability of the Cauchy-Born limit
 682 [11, 3], it follows that $c_{\text{lin}} > 0$. \square

683 As a second corollary, we can even identify the lowest order nonlinearity.

684 COROLLARY 5.5. *In the setting of Section 2.1 assuming additionally the line re-*
 685 *flexion symmetry (15), for W given by (5), one finds $\nabla^3 W(0) = c_{\text{quad}}(E_{111} -$
 686 $3\text{sym } E_{122})$, for some $c_{\text{quad}} \in \mathbb{R}$, and therefore*

$$687 \quad \text{div}(\nabla^3 W(0)[\nabla u, \nabla v]) = c_{\text{quad}} \left(\begin{pmatrix} \partial_{11}v - \partial_{22}v \\ -2\partial_{12}v \end{pmatrix} \cdot \nabla u + \begin{pmatrix} \partial_{11}u - \partial_{22}u \\ -2\partial_{12}u \end{pmatrix} \cdot \nabla v \right).$$

688 *Proof.* As $W(F) = \frac{1}{\det A_\Lambda} V(F \cdot \mathcal{R})$, we have

$$689 \quad \nabla^3 W(0) = \frac{1}{\det A_\Lambda} \sum_{\rho, \sigma, \tau \in \mathcal{R}} \nabla^3 V(0)_{\rho\sigma\tau} \rho \otimes \sigma \otimes \tau.$$

690 Further, due to the rotational symmetry of \mathcal{R} and V , (2), we have $\nabla^3 V(0)_{\rho\sigma\tau} =$
691 $\nabla^3 V(0)_{Q\rho Q\sigma Q\tau}$, hence we can equivalently write

$$692 \quad \nabla^3 W(0) = \frac{1}{\det A_\Lambda} \sum_{\rho, \sigma, \tau \in \mathcal{R}} \nabla^3 V(0)_{\rho\sigma\tau} Q\rho \otimes Q\sigma \otimes Q\tau.$$

693 Furthermore, the line reflection symmetry (15) implies $\nabla^3 V(0)_{\rho\sigma\tau} = -\nabla^3 V(0)_{S\rho S\sigma S\tau}$,
694 which translates to

$$695 \quad \nabla^3 W(0) = -\frac{1}{\det A_\Lambda} \sum_{\rho, \sigma, \tau \in \mathcal{R}} \nabla^3 V(0)_{\rho\sigma\tau} S\rho \otimes S\sigma \otimes S\tau.$$

696 Combining these observations, we find

$$697 \quad \nabla^3 W(0) \in \{A: A = \text{sym } A, Q^{\otimes 3} A = A, S^{\otimes 3} A = -A\},$$

698 and invoking Lemma 5.2, we therefore deduce that

$$\begin{aligned} 699 \quad \nabla^3 W(0) &= \left(\frac{1}{4 \det A_\Lambda} \sum_{\rho, \sigma, \tau \in \mathcal{R}} \nabla^3 V(0)_{\rho\sigma\tau} (\rho_1 \sigma_1 \tau_1 - \rho_1 \sigma_2 \tau_2 - \rho_2 \sigma_1 \tau_2 - \rho_2 \sigma_2 \tau_1) \right) \\ 700 \quad &\cdot (E_{111} - 3 \text{sym } E_{122}) \\ 701 \quad &=: c_{\text{quad}}(E_{111} - 3 \text{sym } E_{122}). \end{aligned}$$

703 Finally, the identity

$$704 \quad \text{div}((E_{111} - 3 \text{sym } E_{122})[\nabla u, \nabla v]) = \begin{pmatrix} \partial_{11} v - \partial_{22} v \\ -2\partial_{12} v \end{pmatrix} \cdot \nabla u + \begin{pmatrix} \partial_{11} u - \partial_{22} u \\ -2\partial_{12} u \end{pmatrix} \cdot \nabla v.$$

705 completes the proof. \square

706 **5.2. Decay of the linear residual.** As discussed in the sketch of the proof, see
707 (14), the crucial object is the *linear residual*

$$708 \quad f_u = -\text{Div}(\nabla^2 V(0)[Du]).$$

709 We now establish how crystalline symmetries lead to a faster decay of f_u as would be
710 expected from linearised elasticity in general.

711 **THEOREM 5.6.** (a) *In the setting of Theorem 2.5, on a square lattice, we*
712 *have*

$$713 \quad |f_{\bar{u}}(x)| \lesssim |x|^{-4}$$

714 *for sufficiently large $|x|$.*

715 (b) *In the setting of Theorem 2.5 on a triangular lattice, we have*

$$\begin{aligned} 716 \quad |f_{\bar{u}}(x)| &\lesssim |x|^{-6} \log^2 |x| + |x|^{-3} |D\bar{u}| + |x|^{-2} |D^2\bar{u}| \\ 717 \quad &\lesssim |x|^{-5} \log |x| \end{aligned}$$

719 *for sufficiently large $|x|$.*

720 (c) In the setting of [Theorem 2.9](#), we have

$$721 \quad |f_{\bar{u}}(x)| \lesssim |x|^{-3}$$

722 for sufficiently large $|x|$. But, writing $\bar{u} = u_1 + u_2 + \bar{u}_{\text{rem}}$ with u_1 and u_2 given
723 by [\(18\)](#) and [\(19\)](#), we have

$$724 \quad |f_{\bar{u}_{\text{rem}}}(x)| \lesssim |D^2 \bar{u}_{\text{rem}}| |D \bar{u}_{\text{rem}}| + |x|^{-2} |D \bar{u}_{\text{rem}}| + |x|^{-1} |D^2 \bar{u}_{\text{rem}}| + |x|^{-5} \\ 725 \lesssim |x|^{-4} \log |x|.$$

727 for sufficiently large $|x|$.

728 *Remark 5.7.* [Theorem 5.6](#) improves on the residual decay estimate $|x|^{-3}$ obtained
729 in [\[8\]](#) in all three cases we consider. This can be used to gain better estimates on \bar{u}
730 or \bar{u}_{rem} which in turn improves the rates here. Iteratively, we will see that the terms
731 involving \bar{u} or \bar{u}_{rem} in all of the above estimates turn out to be negligible.

732 *Proof.* Recall that \bar{u} is a critical point of the energy difference, satisfying the
733 equilibrium equation

$$734 \quad (25) \quad -\text{Div}(\nabla V(D\hat{u} + D\bar{u})) = 0.$$

735 To obtain an estimate on $f_{\bar{u}}(x)$ we first linearise by Taylor expansion of V around 0
736 and then connect to CLE by Taylor expansion of $D\hat{u}$ around x . Note that \hat{u} is not
737 smooth at the branch cut Γ and $D_\rho \hat{u}$ is not close to $\nabla \hat{u} \cdot \rho$ there either. But this
738 is not a problem as the jump of \hat{u} is equal to the periodicity p (or $-p$) of V and
739 $\nabla \hat{u} \in C^\infty(\mathbb{R}^2 \setminus \{0\})$. Therefore, one can always substitute $\hat{u}(x)$ by $\hat{u}(x) \pm p$ where
740 necessary. We will use this implicitly in the following arguments.

741 Taylor expanding V around 0 and ordering by order of decay gives

$$742 \quad 0 = f_{\bar{u}} + I_2 + I_3 + I_4 + I_5 + I_{\text{rem}}$$

743 where

$$744 \quad I_2 = -\text{Div}(\nabla^2 V(0)[D\hat{u}]), \\ 745 \quad I_3 = -\frac{1}{2} \text{Div}(\nabla^3 V(0)[D\hat{u}, D\hat{u}]), \\ 746 \quad I_4 = -\text{Div}(\nabla^3 V(0)[D\hat{u}, D\bar{u}]) - \frac{1}{6} \text{Div}(\nabla^4 V(0)[D\hat{u}, D\hat{u}, D\hat{u}]), \\ 747 \quad I_5 = -\frac{1}{2} \text{Div}(\nabla^3 V(0)[D\bar{u}, D\bar{u}]) - \frac{1}{2} \text{Div}(\nabla^4 V(0)[D\hat{u}, D\hat{u}, D\bar{u}]) \\ 748 \quad - \frac{1}{24} \text{Div}(\nabla^5 V(0)[D\hat{u}]^4), \\ 749$$

750 and the remainder satisfies

$$751 \quad (26) \quad |I_{\text{rem}}| \leq |x|^{-6} \log^2 |x|,$$

752 due to the already known decay estimates on \bar{u} from [Theorem 2.2](#) and the explicit
753 rates for \hat{u} :

$$754 \quad |D^j \hat{u}| \leq |x|^{-j} \quad \text{and} \quad |D^j \bar{u}| \leq |x|^{-j-1} \log |x| \quad \text{for } j \geq 1.$$

755 *Estimate for I_2 :* The term I_2 depends only on \hat{u} . We can expand \hat{u}

$$\begin{aligned}
756 \quad I_2 &= \sum_{\rho, \sigma \in \mathcal{R}} \nabla^2 V(0)_{\rho\sigma} D_{-\sigma} D_{\rho} \hat{u}(x) \\
757 \quad &= \sum_{\rho, \sigma \in \mathcal{R}} \nabla^2 V(0)_{\rho\sigma} (\hat{u}(x + \rho - \sigma) + \hat{u}(x) - \hat{u}(x + \rho) - \hat{u}(x - \sigma)) \\
758 \quad &= J_2 + J_3 + J_4 + J_5 + O(|x|^{-6}),
\end{aligned}$$

760 where

$$\begin{aligned}
761 \quad J_2 &= - \sum_{\rho, \sigma \in \mathcal{R}} \nabla^2 V(0)_{\rho\sigma} \nabla^2 \hat{u}(x) [\rho, \sigma] \\
762 \quad J_3 &= \frac{1}{2} \sum_{\rho, \sigma \in \mathcal{R}} \nabla^2 V(0)_{\rho\sigma} \nabla^3 \hat{u}(x) ([\rho, \sigma, \sigma] - [\rho, \rho, \sigma]) \\
763 \quad J_4 &= \frac{1}{12} \sum_{\rho, \sigma \in \mathcal{R}} \nabla^2 V(0)_{\rho\sigma} \nabla^4 \hat{u}(x) (-2[\rho, \sigma, \sigma, \sigma] + 3[\rho, \rho, \sigma, \sigma] - 2[\rho, \rho, \rho, \sigma]) \\
764 \quad J_5 &= \frac{1}{24} \sum_{\rho, \sigma \in \mathcal{R}} \nabla^2 V(0)_{\rho\sigma} \nabla^5 \hat{u}(x) ([\rho, \sigma, \sigma, \sigma, \sigma] - 2[\rho, \rho, \sigma, \sigma, \sigma] \\
765 \quad &\quad + 2[\rho, \rho, \rho, \sigma, \sigma] - [\rho, \rho, \rho, \rho, \sigma])
\end{aligned}$$

768 Using the symmetry in ρ and σ it follows that $J_3 = J_5 = 0$. By [Lemma 5.2](#),

$$\begin{aligned}
769 \quad (27) \quad J_2 &= - \sum_{\rho, \sigma \in \mathcal{R}} \nabla^2 V(0)_{\rho\sigma} \nabla^2 \hat{u}(x) [\rho, \sigma] \\
770 \quad &= \left(- \sum_{\rho, \sigma \in \mathcal{R}} \nabla^2 V(0)_{\rho\sigma} \rho \otimes \sigma \right) : \nabla^2 \hat{u}(x) \\
771 \quad &= \left(- \frac{1}{2} \sum_{\rho, \sigma \in \mathcal{R}} \nabla^2 V(0)_{\rho\sigma} \rho \cdot \sigma \right) \Delta \hat{u}(x).
\end{aligned}$$

773 Hence, $J_2 = 0$. Thus we conclude so far that $I_2 = J_4 + O(|x|^{-6})$. To proceed, we now
774 distinguish the specific cases we consider.

775 *Proof of (a):* Due to mirror reflection symmetry we have $\nabla^3 V(0) = 0$ and
776 $\nabla^5 V(0) = 0$, hence $I_3 = 0$, $|I_4| \lesssim |x|^{-4}$ and $|I_2| \lesssim |J_4| + |x|^{-6} \lesssim |x|^{-4}$. We therefore
777 obtain $|f_{\bar{u}}| \lesssim |x|^{-4}$ which concludes the proof of (a).

778 *Estimates for J_4, I_4 for cases (b, c):* We use [Lemma 5.2](#) to calculate

$$\begin{aligned}
779 \quad (28) \quad J_4 &= \frac{1}{12} \sum_{\rho, \sigma \in \mathcal{R}} \nabla^2 V(0)_{\rho\sigma} \nabla^4 \hat{u}(x) (-2[\rho, \sigma, \sigma, \sigma] + 3[\rho, \rho, \sigma, \sigma] - 2[\rho, \rho, \rho, \sigma]) \\
780 \quad &= P_{\text{sym}} \left(\frac{1}{12} \sum_{\rho, \sigma \in \mathcal{R}} \nabla^2 V(0)_{\rho\sigma} (-2\rho \otimes \sigma \otimes \sigma \otimes \sigma + 3\rho \otimes \rho \otimes \sigma \otimes \sigma \right. \\
781 \quad &\quad \left. - 2\rho \otimes \rho \otimes \rho \otimes \sigma) : \nabla^4 \hat{u}(x) \right) \\
782 \quad &= \left(\frac{1}{32} \sum_{\rho, \sigma \in \mathcal{R}} \nabla^2 V(0)_{\rho\sigma} (2(\rho \cdot \sigma)^2 + |\rho|^2 |\sigma|^2 - 2\rho \cdot \sigma (|\rho|^2 + |\sigma|^2)) \right) \Delta^2 \hat{u}(x) \\
783 \quad &
\end{aligned}$$

784 As $\Delta^2 \hat{u} = 0$, we find $J_4 = 0$ and hence obtain $|I_2| \lesssim |x|^{-6}$.

785 Next, we consider

$$\begin{aligned}
786 \quad I_4 &= -\frac{1}{6} \operatorname{Div}(\nabla^4 V(0)[D\hat{u}, D\hat{u}, D\hat{u}]) \\
787 \quad &= \frac{1}{6} \sum_{\pi, \rho, \sigma, \tau} \nabla^4 V(0)_{\pi\rho\sigma\tau} D_{-\tau}(D_\pi \hat{u} D_\rho \hat{u} D_\sigma \hat{u}) \\
788 \quad &= -\frac{1}{2} \sum_{\pi, \rho, \sigma, \tau} \nabla^4 V(0)_{\pi\rho\sigma\tau} \nabla^2 \hat{u}[\pi, \tau] \nabla \hat{u} \cdot \rho \nabla \hat{u} \cdot \sigma \\
789 \quad &\quad - \frac{1}{6} \sum_{\pi, \rho, \sigma, \tau} \nabla^4 V(0)_{\pi\rho\sigma\tau} \nabla^3 \hat{u}[\pi, \pi, \tau] \nabla \hat{u} \cdot \rho \nabla \hat{u} \cdot \sigma \\
790 \quad &\quad + \frac{1}{6} \sum_{\pi, \rho, \sigma, \tau} \nabla^4 V(0)_{\pi\rho\sigma\tau} \nabla^3 \hat{u}[\pi, \tau, \tau] \nabla \hat{u} \cdot \rho \nabla \hat{u} \cdot \sigma \\
791 \quad &\quad - \frac{1}{2} \sum_{\pi, \rho, \sigma, \tau} \nabla^4 V(0)_{\pi\rho\sigma\tau} \nabla^2 \hat{u}[\pi, \tau] \nabla^2 \hat{u}[\rho, \rho] \nabla \hat{u} \cdot \sigma \\
792 \quad &\quad + \frac{1}{2} \sum_{\pi, \rho, \sigma, \tau} \nabla^4 V(0)_{\pi\rho\sigma\tau} \nabla^2 \hat{u}[\pi, \tau] \nabla^2 \hat{u}[\rho, \tau] \nabla \hat{u} \cdot \sigma.
\end{aligned}$$

794 The second and third terms cancel each other by symmetry in π and τ , while the
795 fourth and fifth terms both vanish due to $\nabla^4 V(0)_{\pi\rho\sigma\tau} = \nabla^4 V(0)_{(-\pi)(-\rho)(-\sigma)(-\tau)}$.

796 Applying again [Lemma 5.2](#) we can express the first term as

$$\begin{aligned}
797 \quad (29) \quad I_4 &= -\frac{1}{2} \sum_{\pi, \rho, \sigma, \tau} \nabla^4 V(0)_{\pi\rho\sigma\tau} \nabla^2 \hat{u}[\pi, \tau] \nabla \hat{u} \cdot \rho \nabla \hat{u} \cdot \sigma \\
798 \quad &= P_{\text{sym}} \left(-\frac{1}{2} \sum_{\pi, \rho, \sigma, \tau} \nabla^4 V(0)_{\pi\rho\sigma\tau} \pi \otimes \tau \otimes \rho \otimes \sigma \right) : (\nabla^2 \hat{u} \otimes \nabla \hat{u} \otimes \nabla \hat{u}) \\
799 \quad &= \frac{1}{24} \left(-\frac{1}{2} \sum_{\pi, \rho, \sigma, \tau} \nabla^4 V(0)_{\pi\rho\sigma\tau} ((\pi \cdot \tau)(\rho \cdot \sigma) + (\pi \cdot \rho)(\tau \cdot \sigma) + (\pi \cdot \sigma)(\rho \cdot \tau)) \right) \\
800 \quad &\quad \cdot (3\partial_1^2 \hat{u}(\partial_1 \hat{u})^2 + 3\partial_2^2 \hat{u}(\partial_2 \hat{u})^2 + \partial_1^2 \hat{u}(\partial_2 \hat{u})^2 + \partial_2^2 \hat{u}(\partial_1 \hat{u})^2 + 4\partial_1 \partial_2 \hat{u} \partial_1 \hat{u} \partial_2 \hat{u}) \\
801 \quad &= c(|\nabla \hat{u}|^2 \Delta \hat{u} + 2\nabla^2 \hat{u}[\nabla \hat{u}, \nabla \hat{u}]) \\
802 \quad &= c(3|\nabla \hat{u}(x)|^2 + 2)\Delta \hat{u}(x) - 4(1 + |\nabla \hat{u}|^2)^{\frac{3}{2}} H,
\end{aligned}$$

804 where

$$805 \quad H = \frac{(1 + (\partial_1 \hat{u})^2) \partial_2^2 \hat{u} + (1 + (\partial_2 \hat{u})^2) \partial_1^2 \hat{u} - 2\partial_1 \hat{u} \partial_2 \hat{u} \partial_1 \partial_2 \hat{u}}{2(1 + |\nabla \hat{u}|^2)^{\frac{3}{2}}}$$

806 is the mean curvature of the surface given by $x_3 = \hat{u}(x_1, x_2)$. Since the graph of \hat{u} is
807 a helicoid, i.e., a minimal surface, $H \equiv 0$ and therefore we have shown that $I_4 = 0$.

808 *Proof of (b):* Due to the mirror symmetry we again obtain $\nabla^3 V(0) = \nabla^5 V(0) =$
809 0 , hence $I_3 = 0$. In addition, again due to mirror symmetry, I_5 simplifies to

$$810 \quad I_5 = -\frac{1}{2} \operatorname{Div}(\nabla^4 V(0)[D\hat{u}, D\hat{u}, D\bar{u}]).$$

811 Therefore,

$$\begin{aligned}
812 \quad |I_5| &\lesssim |x|^{-3} |D\bar{u}| + |x|^{-2} |D^2 \bar{u}| \\
813 \quad &\lesssim |x|^{-5} \log|x|,
\end{aligned}$$

815 Invoking $I_4 = 0$ and $|I_2| \lesssim |x|^{-6}$ from the previous step concludes the proof of (b).

816 *Proof of (c):* On the BCC lattice, case (c), one typically finds $\nabla^3 V(0) \neq 0$ and
 817 $\nabla^5 V(0) \neq 0$. In particular, I_3 does not vanish, hence our arguments so far only yield
 818 $|f_{\bar{u}}| \leq |x|^{-3}$.

819 To estimate, $f_{\bar{u}_{\text{rem}}}$ we replace \hat{u} with $\hat{u} + u_1 + u_2$ and \bar{u} with \bar{u}_{rem} in the previous
 820 steps of the proof. Recall from (20) that $|\nabla^j u_i| \lesssim |x|^{-i-j}$.

821 Clearly, Equation (25) and the Taylor expansion of V including (26) still hold.
 822 For the estimates let us start with the higher order terms. We can estimate directly

$$823 \quad |-\text{Div}(\nabla^3 V(0)[D(\hat{u} + u_1 + u_2), D\bar{u}_{\text{rem}}])| \leq |x|^{-2}|D\bar{u}_{\text{rem}}| + |x|^{-1}|D^2\bar{u}_{\text{rem}}|.$$

824 If we also substitute \hat{u} by $\hat{u} + u_1 + u_2$ in (29), we find overall that

$$825 \quad |I_4| \lesssim |x|^{-2}|D\bar{u}_{\text{rem}}| + |x|^{-1}|D^2\bar{u}_{\text{rem}}| + |x|^{-5} \\ 826 \quad \lesssim |x|^{-4} \log|x|.$$

828 In the same spirit we estimate

$$829 \quad |I_5| \lesssim |D^2\bar{u}_{\text{rem}}||D\bar{u}_{\text{rem}}| + |x|^{-3}|D\bar{u}_{\text{rem}}| + |x|^{-2}|D^2\bar{u}_{\text{rem}}| + |x|^{-5} \\ 830 \quad \lesssim |x|^{-5} \log^2|x|.$$

832 The important difference to before are found in I_2 and I_3 . Let us start with I_2 . As
 833 before, we find $J_3 = J_5 = 0$. Substituting \hat{u} by $\hat{u} + u_1 + u_2$ in (28), we estimate

$$834 \quad |J_4| \lesssim |\Delta^2(\hat{u} + u_1 + u_2)| = |\Delta^2(u_1 + u_2)| \lesssim |x|^{-5}.$$

835 Therefore, $I_2 = J_2 + O(|x|^{-5})$. It is crucial that now J_2 does not vanish to be able to
 836 cancel out the first terms in the nonlinearity I_3 . Following (27), we have

$$837 \quad J_2 = - \sum_{\rho, \sigma \in \mathcal{R}} \nabla^2 V(0)_{\rho\sigma} \nabla^2(u_1 + u_2)(x)[\rho, \sigma] \\ 838 \quad = - \det(A_\Lambda) \text{div}(\nabla^2 W(0)[\nabla(u_1 + u_2)]) \\ 839 \quad = - \det(A_\Lambda) c_{\text{lin}} \Delta(u_1 + u_2)$$

841 Now let us come to I_3 . Clearly,

$$842 \quad I_3 = -\frac{1}{2} \text{Div}(\nabla^3 V(0)[D\hat{u}, D\hat{u}]) \\ 843 \quad - \text{Div}(\nabla^3 V(0)[D\hat{u}, Du_1]) + O(|x|^{-5}).$$

845 Developing the discrete differences as we did previously for I_2 , we find

$$846 \quad - \text{Div}(\nabla^3 V(0)[D\hat{u}, Du_1]) \\ 847 \quad = \sum_{\rho, \sigma, \tau \in \mathcal{R}} \nabla^3 V(0)_{\sigma\rho\tau} D_{-\tau}(D_\rho \hat{u}(x) D_\sigma u_1(x)) \\ 848 \quad = - \sum_{\rho, \sigma, \tau \in \mathcal{R}} \nabla^3 V(0)_{\sigma\rho\tau} (\nabla \hat{u}(x)[\rho] \nabla^2 u_1(x)[\sigma, \tau] + \nabla u_1(x)[\sigma] \nabla^2 \hat{u}(x)[\rho, \tau]) \\ 849 \quad + O(|x|^{-5}) \\ 850 \quad = - \det A_\Lambda \text{div}(\nabla^3 W(0)[\nabla \hat{u}, \nabla u_1]) + O(|x|^{-5}).$$

852 For the other term we have to take a few more terms into account. For those we again
 853 use the fact that $\nabla^3 V(0)_{\sigma\rho\tau} = -\nabla^3 V(0)_{(-\sigma)(-\rho)(-\tau)}$.

$$\begin{aligned}
 854 & -\frac{1}{2} \operatorname{Div}(\nabla^3 V(0)[D\hat{u}, D\hat{u}]) \\
 855 & = \frac{1}{2} \sum_{\rho, \sigma, \tau \in \mathcal{R}} \nabla^3 V(0)_{\sigma\rho\tau} D_{-\tau}(D_\rho \hat{u}(x) D_\sigma \hat{u}(x)) \\
 856 & = \frac{1}{2} \sum_{\rho, \sigma, \tau \in \mathcal{R}} \nabla^3 V(0)_{\sigma\rho\tau} (D_{-\tau} D_\rho \hat{u}(x) D_\sigma \hat{u}(x) + D_\rho \hat{u}(x - \tau) D_{-\tau} D_\sigma \hat{u}(x)) \\
 857 & = \frac{1}{2} \sum_{\rho, \sigma, \tau \in \mathcal{R}} \nabla^3 V(0)_{\sigma\rho\tau} \left(-2\nabla \hat{u}(x)[\sigma] \nabla^2 \hat{u}(x)[\rho, \tau] \right. \\
 858 & \quad \left. + (\nabla^3 \hat{u}(x)[\rho, \tau, \tau] - \nabla^3 \hat{u}(x)[\rho, \rho, \tau]) \nabla \hat{u}(x)[\sigma] - \nabla^2 \hat{u}(x)[\rho, \tau] \nabla^2 \hat{u}(x)[\sigma, \sigma] \right. \\
 859 & \quad \left. + \nabla^2 \hat{u}(x)[\rho, \tau] \nabla^2 \hat{u}(x)[\sigma, \tau] \right) + O(|x|^{-5}) \\
 860 & = - \sum_{\rho, \sigma, \tau \in \mathcal{R}} \nabla^3 V(0)_{\sigma\rho\tau} \nabla \hat{u}(x)[\sigma] \nabla^2 \hat{u}(x)[\rho, \tau] + O(|x|^{-5}) \\
 861 & = -\det A_\Lambda \frac{1}{2} \operatorname{div}(\nabla^3 W(0)[\nabla \hat{u}, \nabla \hat{u}]) + O(|x|^{-5}) \\
 862 &
 \end{aligned}$$

863 Hence, we can use [Equations \(16a\)](#) and [\(16b\)](#) for u_1 and u_2 to conclude that $J_2 + I_3 =$
 864 $O(|x|^{-5})$. This concludes the proof. \square

865 **5.3. Proofs of the main theorems.** The connection between the decay of f_u
 866 and the decay of u is as follows:

867 **THEOREM 5.8.** *Let $u \in \dot{\mathcal{H}}^1$, and $j \in \{1, 2\}$.*

868 (a) *If $|f_u(x)| \lesssim |x|^{-3}$ and $\sum_x f_u = 0$, then for $|x|$ sufficiently large,*

$$869 \quad |D^j u(x)| \lesssim |x|^{-1-j} \log|x|.$$

870 (b) *If $|f_u(x)| \lesssim |x|^{-4}$, $\sum_x f_u = 0$, and $\sum_x f_u x = 0$, then for $|x|$ sufficiently large,*

$$871 \quad |D^j u(x)| \lesssim |x|^{-2-j} \log|x|.$$

872 (c) *If $|f_u(x)| \lesssim |x|^{-5}$, $\sum_x f_u = 0$, $\sum_x f_u x = 0$, and $\sum_x f_u x \otimes x \propto \operatorname{Id}$, then for
 873 $|x|$ sufficiently large,*

$$874 \quad |D^j u(x)| \lesssim |x|^{-3-j} \log|x|.$$

875 (d) *If the assumptions on the decay rate of f_u in (a), (b), or (c) are slightly
 876 stronger, namely $|x|^{-3-\varepsilon}$, $|x|^{-4-\varepsilon}$, or $|x|^{-5-\varepsilon}$ for some $\varepsilon > 0$, then the result-
 877 ing rates for $D^j u$ are true without the logarithmic term, i.e. $|x|^{-1-j}$, $|x|^{-2-j}$,
 878 and $|x|^{-3-j}$, respectively.*

879 *Proof.* Statement (a) is part of the results in [8]. Its extensions (b), (c), and (d)
 880 follow a similar basic strategy. The approach is based on knowledge about the lattice
 881 Green's function G as one can write Du as a convolution on the lattice, $Du = f_u *_\Lambda DG$,
 882 that is,

$$883 \quad Du(x) = \sum_{z \in \Lambda} f_u(z) DG(x - z).$$

884 The proof of (b), (c), and (d) is part of a full theory developed in [2]. All the details
 885 as well as further generalisations will be presented there. \square

886 **Theorem 5.8** shows that, to prove the main results in **Sections 2.2** and **2.3**, in
 887 addition to the decay of f_u established in **Section 5.2**, we also need to analyse its
 888 moments.

889 **THEOREM 5.9.** *In the setting of **Section 2.1**. Let $[u] \in \dot{\mathcal{H}}^1$ inherit the rotational
 890 symmetry (11) and let f_u denote the resultant linear residual (14). Then we have
 891 $\sum_x f_u = 0$, $\sum_x f_u x = 0$, and $\sum_x f_u x \otimes x = c \text{Id}$ for some $c \in \mathbb{R}$, provided the sums
 892 converge absolutely.*

893 *Proof.* We begin with $\sum_x f_u = 0$. A version of this statement is already needed
 894 in **Proposition 2.1** since it is directly linked with the net-force of the system. **Propo-**
 895 **sition 2.1** was established in [8]. As there was a gap in the proof, namely a proof of
 896 the specific claim $\sum_x f_u = 0$ in question here, let us give the details in our specific
 897 case: Let η be a smooth cut-off function with $\eta(x) = 1$ for $|x| \leq 1$ and $\eta(x) = 0$ for
 898 $|x| \geq 2$ and let $\eta_M(x) = \eta(\frac{x}{M})$. Then we have

$$\begin{aligned}
 899 \quad \sum_x f_u &= \lim_{M \rightarrow \infty} \sum_x f_u \eta_M \\
 900 \quad &= \lim_{M \rightarrow \infty} \sum_x \text{Div} (\nabla V(D\hat{u} + Du) - \nabla V(0) - \nabla^2 V(0)[D\hat{u} + Du]) \eta_M \\
 901 \quad &\quad + \lim_{M \rightarrow \infty} \sum_x \text{Div} \nabla^2 V(0)[D\hat{u}] \eta_M \\
 902 \quad &= - \lim_{M \rightarrow \infty} \sum_x (\nabla V(D\hat{u} + Du) - \nabla V(0) - \nabla^2 V(0))[D\hat{u} + Du][D\eta_M] \\
 903 \quad &\quad - \lim_{M \rightarrow \infty} \sum_x \nabla^2 V(0)[D\hat{u}, D\eta_M] \\
 904 \quad &=: \lim_{M \rightarrow \infty} A_M + B_M. \\
 905
 \end{aligned}$$

906 Since the support of $D\eta_M$ is contained in $\{x: M - C \leq |x| \leq 2M + C\}$, for
 907 some fixed $C > 0$, the first term, A_M , can be estimated as a remainder in a Taylor
 908 expansion by

$$\begin{aligned}
 909 \quad |A_M| &= \left| \sum_x (\nabla V(D\hat{u} + Du) - \nabla V(0) - \nabla^2 V(0))[D\hat{u} + Du][D\eta_M] \right| \\
 910 \quad &\lesssim \sum_x |D\hat{u} + Du|^2 |D\eta_M| \\
 911 \quad &\lesssim M^2 M^{-3} + \|u\|_{\dot{\mathcal{H}}^1}^2 M^{-1} \\
 912 \quad &\lesssim M^{-1}.
 \end{aligned}$$

914 For the second term, B_M , note that $M - C \leq |x| \leq 2M + C$ implies $D\hat{u} = \nabla \hat{u} \cdot \mathcal{R} +$
 915 $O(M^{-2})$ and $D\eta_M = \nabla \eta_M \cdot \mathcal{R} + O(M^{-2})$. Estimating also the ‘‘quadrature error’’
 916 (replacing the sum by an integral) we obtain

$$\begin{aligned}
 917 \quad B_M &= \frac{1}{\det A_\Lambda} \int_{\mathbb{R}^2} \nabla^2 V(0)[\nabla \hat{u} \cdot \mathcal{R}, \nabla \eta_M \cdot \mathcal{R}] + O(M^{-1}) \\
 918 \quad &= \int_{\mathbb{R}^2 \setminus B_1(0)} \nabla^2 W(0)[\nabla \hat{u}, \nabla \eta_M] + O(M^{-1}), \\
 919
 \end{aligned}$$

920 where we used the fact that $\nabla \eta_M = 0$ on $B_1(0)$ for M sufficiently large. Applying

921 Gauß's theorem as well as the fact that $\nabla\hat{u}(x)$ is always orthogonal to ν , we obtain

$$\begin{aligned}
922 \quad B_M &= \int_{\partial B_1(\hat{x})} \nabla^2 W(0) [\nabla\hat{u}] \cdot \nu \, dS(x) + O(M^{-1}) \\
923 \quad &= c_{\text{lin}} \int_{\partial B_1(\hat{x})} \nabla\hat{u} \cdot \nu \, dS(x) + O(M^{-1}) \\
924 \quad &= O(M^{-1}).
\end{aligned}$$

926 Thus, we have shown that

$$927 \quad \sum_x f_u = \lim_{M \rightarrow \infty} (A_M + B_M) = 0.$$

928 To prove our claims about the first and second moments, we first show that
929 rotational symmetry of \bar{u} implies rotational symmetry of f_u , i.e., $f_u(L_Q x) = f_u(x)$:

$$\begin{aligned}
930 \quad f_u(L_Q x) &= \sum_{\rho, \sigma \in \mathcal{R}} \nabla^2 V(0)_{\rho, \sigma} (D_\sigma u(L_Q x - \rho) - D_\sigma u(L_Q x)) \\
931 \quad &= \sum_{\rho, \sigma \in \mathcal{R}} \nabla^2 V(0)_{Q\rho, Q\sigma} (D_{Q\sigma} u(L_Q x - Q\rho) - D_{Q\sigma} u(L_Q x)) \\
932 \quad &= \sum_{\rho, \sigma \in \mathcal{R}} \nabla^2 V(0)_{Q\rho, Q\sigma} (D_{Q\sigma} u(L_Q(x - \rho)) - D_{Q\sigma} u(L_Q x)) \\
933 \quad &= \sum_{\rho, \sigma \in \mathcal{R}} \nabla^2 V(0)_{Q\rho, Q\sigma} (D_\sigma u(x - \rho) - D_\sigma u(x)) \\
934 \quad &= \sum_{\rho, \sigma \in \mathcal{R}} \nabla^2 V(0)_{\rho, \sigma} (D_\sigma u(x - \rho) - D_\sigma u(x)) \\
935 \quad &= f_u(x),
\end{aligned}$$

937 where we have used $Q\mathcal{R} = \mathcal{R}$, $D_\sigma u(x) = D_{Q\sigma} u(L_Q x)$, as well as the rotational
938 symmetry of V , (2). Let $N = 3$ for the triangular lattice and $N = 4$ for the quadratic
939 lattice, then

$$\begin{aligned}
940 \quad \sum_x f_u(x)x &= \sum_x f_u(x)(x - \hat{x}) \\
941 \quad &= \frac{1}{N} \sum_x \sum_{j=0}^{N-1} f_u(L_Q^j x) Q^j(x - \hat{x}) \\
942 \quad &= \frac{1}{N} \sum_x f_u(x) \sum_{j=0}^{N-1} Q^j(x - \hat{x}) \\
943 \quad &= 0
\end{aligned}$$

945 and similarly for the second moment,

$$\begin{aligned}
946 \quad \sum_x f_u(x)x \otimes x &= \sum_x f_u(x)(x - \hat{x}) \otimes (x - \hat{x}) \\
947 \quad &= \frac{1}{N} \sum_x \sum_{j=0}^{N-1} f_u(L_Q^j x)(Q^j(x - \hat{x})) \otimes (Q^j(x - \hat{x})) \\
948 \quad &= \sum_x f_u(x)P((x - \hat{x}) \otimes (x - \hat{x})) \\
949 \quad &= \text{Id} \left(\frac{1}{2} \sum_x f_u(x)|x - \hat{x}|^2 \right) \\
950
\end{aligned}$$

951 where we used [Lemma 5.2](#) in the last step. \square

952 Finally, we can combine all the foregoing results to prove our main theorems.

953 *Proof of [Theorem 2.5](#).* Let us start with the square lattice. According to [Theorem](#)
954 [5.6](#), we have $|f_{\bar{u}}| \lesssim |x|^{-4}$. In particular, $\sum_x f_{\bar{u}}$ and $\sum_x f_{\bar{u}}x$ converge. Due to
955 [Theorem 5.9](#), $\sum_x f_{\bar{u}} = 0$ and $\sum_x f_{\bar{u}}x = 0$. Hence, by [Theorem 5.8](#)

$$956 \quad |D^j \bar{u}(x)| \lesssim |x|^{-2-j} \log|x|.$$

957 for $j = 1, 2$ and $|x|$ large enough.

958 For the triangular lattice [Theorem 5.6](#) gives us $|f_{\bar{u}}| \lesssim |x|^{-5} \log|x| \lesssim |x|^{-4-\varepsilon}$. In
959 particular, $\sum_x f_{\bar{u}}$, $\sum_x f_{\bar{u}}$, and $\sum_x f_{\bar{u}}x \otimes x$ converge. Due to [Theorem 5.9](#), $\sum_x f_{\bar{u}} = 0$,
960 $\sum_x f_{\bar{u}}x = 0$, and $\sum_x f_{\bar{u}}x \otimes x = c \text{Id}$. At first, by [Theorem 5.8](#) we conclude that

$$961 \quad |D^j \bar{u}(x)| \lesssim |x|^{-2-j}.$$

962 for $j = 1, 2$ and $|x|$ large enough. But then [Theorem 5.6](#) gives the stronger result
963 $|f_{\bar{u}}| \lesssim |x|^{-6} \log^2|x| \leq |x|^{-5-\varepsilon}$, so that by [Theorem 5.8](#) we indeed get

$$964 \quad |D \bar{u}(x)| \lesssim |x|^{-3-j}$$

965 for $j = 1, 2$ and $|x|$ large enough. \square

966 *Proof of [Theorem 2.9](#).* As in the triangular lattice case we have to argue in several
967 steps. As a starting point [Theorem 5.6](#) shows that $|f_{\bar{u}_{\text{rem}}}| \lesssim |x|^{-4} \log|x| \leq |x|^{-3-\varepsilon}$.
968 In particular, $\sum_x f_{\bar{u}_{\text{rem}}}$ and $\sum_x f_{\bar{u}_{\text{rem}}}x$ converge. Due to [Theorem 5.9](#), $\sum_x f_{\bar{u}_{\text{rem}}} = 0$
969 and $\sum_x f_{\bar{u}_{\text{rem}}}x = 0$. With [Theorem 5.8](#) we find

$$970 \quad |D^j \bar{u}_{\text{rem}}(x)| \lesssim |x|^{-1-j}$$

971 for $j = 1, 2$, which in turn gives the improved estimate $|f_{\bar{u}_{\text{rem}}}| \lesssim |x|^{-4}$ in [Theorem 5.6](#).
972 Going back to [Theorem 5.8](#) we now get

$$973 \quad |D^j \bar{u}_{\text{rem}}(x)| \lesssim |x|^{-2-j} \log|x|.$$

974 Another iteration of [Theorems 5.6](#) and [5.8](#) improves this to

$$975 \quad |D^j \bar{u}_{\text{rem}}(x)| \lesssim |x|^{-2-j}.$$

976 Finally, by [Theorem 5.6](#), we now find $|f_{\bar{u}_{\text{rem}}}| \lesssim |x|^{-5}$. In particular, $\sum_x f_{\bar{u}_{\text{rem}}}x \otimes x$
977 converges as well and due to [Theorem 5.9](#), $\sum_x f_{\bar{u}_{\text{rem}}}x \otimes x = c \text{Id} = c' \nabla^2 W(0)$. A last
978 use of [Theorem 5.8](#) gives the desired result,

$$979 \quad |D^j \bar{u}_{\text{rem}}(x)| \lesssim |x|^{-3-j} \log|x|$$

980 for $j = 1, 2$ and $|x|$ large enough. \square

981 **Acknowledgements.** We thank Tom Hudson and Petr Grigorev for insightful
 982 discussions on symmetries of screw dislocations in BCC.

983 REFERENCES

- 984 [1] R. ALICANDRO, L. DE LUCA, A. GARRONI, AND M. PONSIGLIONE, *Metastability and dynamics*
 985 *of discrete topological singularities in two dimensions: A γ -convergence approach*, Archive
 986 for Rational Mechanics and Analysis, 214 (2014), pp. 269–330, [https://doi.org/10.1007/](https://doi.org/10.1007/s00205-014-0757-6)
 987 [s00205-014-0757-6](https://doi.org/10.1007/s00205-014-0757-6).
- 988 [2] J. BRAUN, T. HUDSON, AND C. ORTNER. in preparation.
- 989 [3] J. BRAUN AND B. SCHMIDT, *Existence and convergence of solutions of the boundary value prob-*
 990 *lem in atomistic and continuum nonlinear elasticity theory*, Calculus of Variations and Par-
 991 tial Differential Equations, 55 (2016), p. 125, <https://doi.org/10.1007/s00526-016-1048-x>.
- 992 [4] H. CHEN AND C. ORTNER, *QM/MM methods for crystalline defects. Part 1: Locality of*
 993 *the tight binding model*, Multiscale Model. Simul., 14(1) (2016), [https://doi.org/10.1137/](https://doi.org/10.1137/15M1022628)
 994 [15M1022628](https://doi.org/10.1137/15M1022628).
- 995 [5] H. CHEN AND C. ORTNER, *QM/MM methods for crystalline defects. Part 2: Consistent energy*
 996 *and force-mixing*, Multiscale Model. Simul., 15(1) (2017).
- 997 [6] W. E AND P. MING, *Cauchy-Born rule and the stability of crystalline solids: Static prob-*
 998 *lems*, Arch. Rational Mech. Anal., 183 (2007), pp. 241–297, [https://doi.org/10.1007/](https://doi.org/10.1007/s00205-006-0031-7)
 999 [s00205-006-0031-7](https://doi.org/10.1007/s00205-006-0031-7).
- 1000 [7] V. EHRLACHER, C. ORTNER, AND A. V. SHAPEEV, *Analysis of boundary conditions for crystal*
 1001 *defect atomistic simulations (preprint)*, <https://arxiv.org/abs/1306.5334>.
- 1002 [8] V. EHRLACHER, C. ORTNER, AND A. V. SHAPEEV, *Analysis of boundary conditions for crystal*
 1003 *defect atomistic simulations*, Archive for Rational Mechanics and Analysis, 222 (2016),
 1004 pp. 1217–1268, <https://doi.org/10.1007/s00205-016-1019-6>.
- 1005 [9] J. P. HIRTH AND J. LOTHE, *Theory of dislocations*, New York Wiley, second ed., 1982.
- 1006 [10] T. HUDSON, *Upscaling a model for the thermally-driven motion of screw dislocations*, Archive
 1007 for Rational Mechanics and Analysis, 224 (2017), pp. 291–352, [https://doi.org/10.1007/](https://doi.org/10.1007/s00205-017-1076-5)
 1008 [s00205-017-1076-5](https://doi.org/10.1007/s00205-017-1076-5).
- 1009 [11] T. HUDSON AND C. ORTNER, *On the stability of Bravais lattices and their Cauchy-Born*
 1010 *approximations*, ESAIM:M2AN, 46 (2012), pp. 81–110, [https://doi.org/10.1051/m2an/](https://doi.org/10.1051/m2an/2011014)
 1011 [2011014](https://doi.org/10.1051/m2an/2011014).
- 1012 [12] T. HUDSON AND C. ORTNER, *Existence and stability of a screw dislocation under anti-plane*
 1013 *deformation*, Archive for Rational Mechanics and Analysis, 213 (2014), pp. 887–929, <https://doi.org/10.1007/s00205-014-0746-9>.
- 1014 [13] M. ITAKURA, H. KABURAKI, M. YAMAGUCHI, AND T. OKITA, *The effect of hydrogen atoms*
 1015 *on the screw dislocation mobility in bcc iron: A first-principles study*, Acta Materialia, 61
 1016 (2013), pp. 6857–6867, <https://doi.org/10.1016/j.actamat.2013.07.064>.
- 1017 [14] L. D. LANDAU AND E. M. LIFSHITZ, *Theory of Elasticity*, Volume 7 of Course of Theoretical
 1018 Physics, Pergamon Press, second english edition ed., 1959. Translated from the Russian
 1019 by J.B. Sykes and W. H. Reid.
- 1020 [15] M. LUSKIN AND C. ORTNER, *Atomistic-to-continuum-coupling*, Acta Numerica, (2013), <https://doi.org/10.1017/S0962492913000068>.
- 1021 [16] C. ORTNER AND F. THEIL, *Justification of the Cauchy-Born approximation of elastodynam-*
 1022 *ics*, Arch. Rational Mech. Anal., 207 (2013), pp. 1025–1073, [https://doi.org/10.1007/](https://doi.org/10.1007/s00205-012-0592-6)
 1023 [s00205-012-0592-6](https://doi.org/10.1007/s00205-012-0592-6).
- 1024 [17] D. PACKWOOD, J. KERMODE, L. MONES, N. BERNSTEIN, J. WOOLLEY, N. GOULD, C. OR-
 1025 *TNER, AND G. CSÁNYI, A universal preconditioner for simulating condensed phase mate-*
 1026 *rials*, The Journal of Chemical Physics, 144 (2016), p. 164109, [https://doi.org/10.1063/1.](https://doi.org/10.1063/1.4947024)
 1027 [4947024](https://doi.org/10.1063/1.4947024).
- 1028 [18] M. PONSIGLIONE, *Elastic energy stored in a crystal induced by screw dislocations: From dis-*
 1029 *crete to continuous*, SIAM J Math Anal, 39 (2007), pp. 449–469, [https://doi.org/10.1137/](https://doi.org/10.1137/060657054)
 1030 [060657054](https://doi.org/10.1137/060657054).
- 1031 [19] J. WANG, Y. L. ZHOU, M. LI, AND Q. HOU, *A modified W–W interatomic potential based*
 1032 *on ab initio calculations*, Modelling and Simulation in Materials Science and Engineering,
 1033 22 (2014), p. 015004, <https://doi.org/10.1088/0965-0393/22/1/015004>.
- 1034
- 1035